Vapour-liquid equilibrium study of tertiary amines, single and in blend with 3-(methylamino)propylamine, for post-combustion CO_2 capture

Ida M. Bernhardsen [a], Anastasia A. Trollebø [a], Cristina Perinu [b], Hanna K. Knuutila [a,⇑]

[a] *Department of Chemical Engineering, Norwegian University of Science and Technology (NTNU), NO-7491 Trondheim, Norway*
[b] *Department of Process, Energy and Environmental Technology, University of Southeast Norway, Post Box 235, NO-3603 Kongsberg, Norway*

a b s t r a c t

This work studies the potential of using the tertiary amines 3-dimethylamino-1-propanol (3DMA1P), 3- diethylamino-1-propanol (3DEA1P) and 1-(2-hydroxyethyl)pyrrolidine (1-(2HE)PRLD) as an alternative to 2-(diethylamino)ethanol (DEEA) in the blend with 3-(methylamino)propylamine (MAPA). Vapour pressure of the three tertiary amines and vapour-liquid equilibrium (VLE) of the binary mixtures 3DMA1P/H_2O, 3DEA1P/H_2O and 1-(2HE)PRLD/H_2O at T= (353, 363 and 373) K were measured in a mod- ified Swietoslawski ebulliometer. The vapour pressure of the pure amines was fitted to the Antoine equa- tion, and the *P-T-x-y* data were fitted to NRTL equations. VLE of the CO_2 loaded blended amines were measured in the temperature range of T = 313 to 393 K, and speciation data of equilibrated samples at different CO_2 loadings were obtained by NMR spectroscopy.

The study showed that the tertiary amines 3DMA1P, 3DEA1P and 1-(2HE)PRLD in the binary amine/ H_2O system were less volatile than DEEA in aqueous solution. The CO_2 loaded blended amines showed comparable VLE behaviour, as well as speciation, and obtained a cyclic capacity higher than that of 30 wt% MEA but similar to most of the blended amines studied in the literature. The overall results indi- cated that the tertiary amines studied in this work can be used as an alternative to DEEA.

1. Introduction

Significant reduction in the world's emissions of CO_2 and other greenhouse gases are needed to limit global temperature rise to below 2 Celsius. One of the technologies that can be used to reach this goal is carbon capture and storage (CCS) [1]. CCS systems capture CO_2 from energy and industrial sources and permanently store CO_2 in geological formations. Among the capture technologies for post-combustion CO_2 capture, amine-based chemical absorption is regarded as the most feasible, but it suffers from various drawbacks such as unfavourable thermodynamics and solvent degradation. To make the technology commercially available, it has to become economically attractive and at the same time contribute to low or no negative environmental impact. One way to address this issue is to search for solvents that have favourable characteristics for energy requirement, reaction rate and are stable at process conditions. Primary and secondary amines, which react with CO_2 to form amine carbamate (Eq. (1)), are characterized by fast absorption rate and high heat of absorption, while tertiary amines, which promote the formation of (bi)carbonate (Eq. (2)), are charac- terized by a slow reaction rate and low heat of absorption.

$$CO_2 + 2RNH_2 \leftrightarrow RNHCOO^- + RNH_3^+ \quad (1)$$

$$CO_2 + R_3N + H_2O \leftrightarrow HCO_3^- + R_3NH^+ \quad (2)$$

In the literature, a substantial number of studies focus on aqueous blends of primary/secondary and tertiary amines as they in the mixture will have relatively high absorption rate and cyclic capacity, and low heat of absorption [2]. A solvent with high cyclic capacity would be an advantage as it reduces the sensible heat loss and results in a smaller circulation flow rate. In Fig. 1, the cyclic capacity of 17 blended amines and the benchmark solvent 30 wt % MEA are compared [3–10]. The cyclic capacity was estimated as given in Eq. (3) by collecting available VLE data at a relevant temperature and partial pressure of CO_2. This can be considered as an optimistic way to calculate cyclic capacity as the bottom of the absorber is likely at a higher temperature than 313 K, but this temperature is commonly used in the literature [11–13]. From the figure, it can be seen that the blended amines show higher cyclic capacity than 30 wt% MEA, and all blends are below a cyclic capacity of 2.6 molCO_2 $kg_{solution}^{-1}$. Also, the cyclic capacity increased with

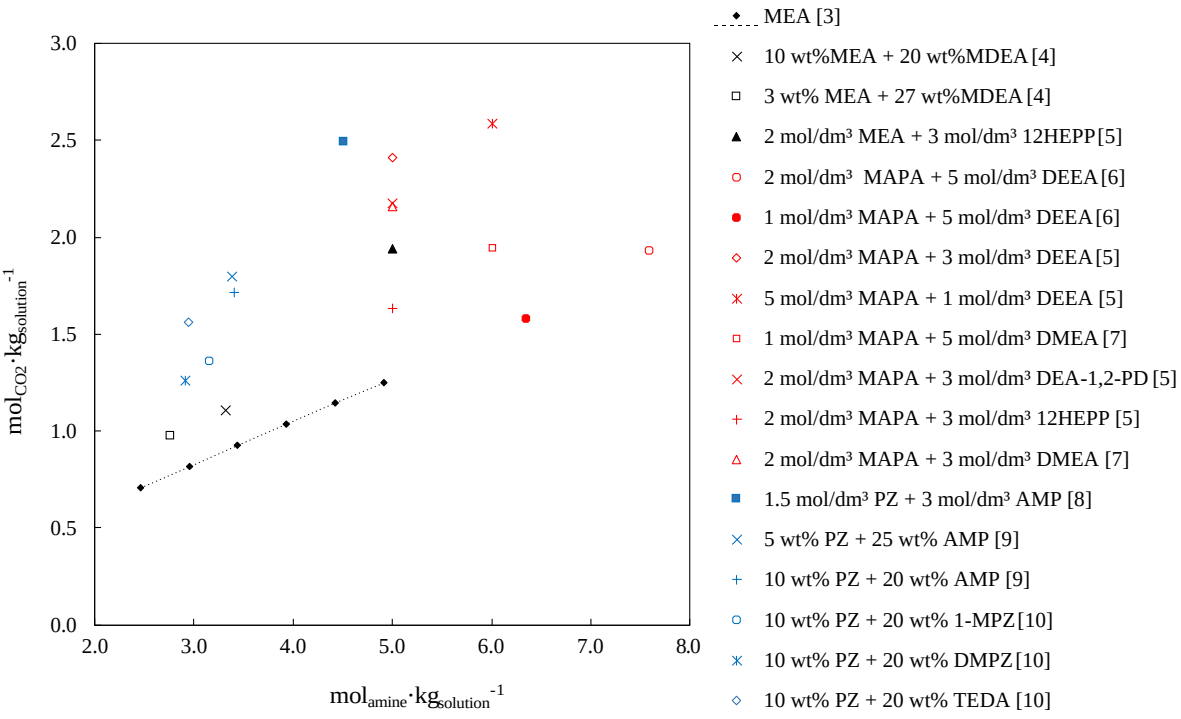

Fig. 1. Estimated cyclic capacity of blended amine solvents using Eq. (3).

increasing solvent concentration. However, a high solvent concentration is not always an advantage as it may lead to higher viscosity, foaming issues and cause solvation problems.

Despite great interest in blended amines as an absorbent for CO_2 capture, Fig. 1 also reflects that few VLE studies have been conducted at temperatures realistic for the desorption process (T = 393 K). Commonly, VLE studies for blended amines are available in the temperature range of 313 K to 353 K [14–18]. VLE data over a wide range of temperatures, pressures and concentrations are essential for the process design, optimisation and simulation of the CO_2 capture plant, and to make a proper choice of absorbent.

cyclic capacity ¼ α_{rich}ðT ¼ 313 K; P_{CO2} ¼ 9:5 kPaÞ
— α_{lean}ðT ¼ 393 K; P_{CO2} ¼ 20:0 kPaÞ ð3Þ

A blended amine solvent which has been extensively studied on lab-scale and tested in a pilot plant campaign is the aqueous solution of 2-(diethylamino)ethanol (DEEA) and 3-(methylamino) propylamine (MAPA) [19–24]. DEEA has been used because of its low heat of absorption and MAPA because of its fast reaction rate with CO_2. Monteiro et al. [25] reported that the CO_2 absorption rate in MAPA was almost twice as fast as piperazine (PZ) and 15 times faster than MEA. However, due to the relatively high volatility of DEEA, it is desirable to replace DEEA with a less volatile tertiary amine [23]. For this reason, a previous work studied ten tertiary amines blended with MAPA using the fast solvent screening method [26]. The result indicated that, in the blend with MAPA, the optimum pKa value of the tertiary amine, giving the highest cyclic capacity, was between pKa 9.48 and 10.13. Based on this work, three tertiary amines were selected for further study: 3-dimethylamino-1-propanol (3DMA1P), 1-(2-hydroxyethyl) pyrrolidine (1-(2HE)PRLD) and 3-diethylamino-1-propanol (3DEA1P) (Fig. 2). In the literature, both 3DMA1P and 1-(2HE) PRLD have been suggested as potential tertiary amines to be used in a blended system. The tertiary amine 3DMA1P is reported to have high absorption capacity [27,28] and similar heat of absorption as the commonly used tertiary amine MDEA [29,30]. Kadiwala et al. [31] reported that the reaction rate of CO_2 in aqueous solutions of 3DMA1P was faster than that of methyldiethanolamine (MDEA) and two times faster than that of the isomer 1-dimethylamino-2-propanol (1DMA2P). Further, the density of unloaded and CO_2 loaded aqueous 3DMA1P solutions was measured by Idris et al. [32], and vapour pressure data of 3DMA1P and binary VLE data of the 3DMA1P/H_2O system were reported

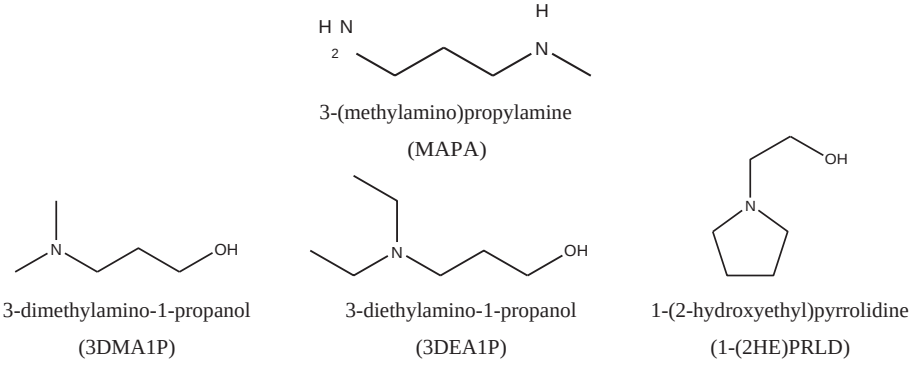

Fig. 2. Molecular structure of the amines studied in this work.

by Belabbaci et al. [33]. Regarding 1-(2HE)PRLD, the amine is reported to have faster reaction kinetics than MDEA and high absorption capacity [34]. Hartono et al. [35] characterised 40 wt% 1-(2HE)PRLD aqueous solution by measuring VLE in the temperature range of 313–393 K, and density and viscosity of unloaded and CO_2 loaded solutions. In addition, the tertiary amine was tested for thermal and oxidative degradation, ecotoxicity and biodegradation. The study reported that 1-(2HE)PRLD was non-toxic (EC_{50} < 10 mg/L), biodegradable (BOD > 20%) and more stable toward degradation than MEA.

This work studies the possibility of using the three tertiary amines 3DMA1P, 3DEA1P and 1-(2HE)PRLD as an alternative to DEEA in the blend with MAPA as solvents for post-combustion CO_2 capture. Vapour pressure of the three alkanolamines and binary VLE of 3DMA1P/H_2O, 3DEA1P/H_2O and 1-(2HE)PRLD/H_2O were measured using a modified Swietoslawski ebulliometer. The vapour pressures were fitted to the Antoine equation and the NRTL-model was used to represent the experimental *P-T-x-y* data. In addition, VLE data for the CO_2 loaded blended amines were reported in the temperature range of 313–393 K and fitted to a simplified VLE model. The results were supported by speciation data obtained using NMR spectroscopy.

2. Materials and methods

2.1. Materials

Chemicals used in this work are listed in Table 1. All chemicals were used without further purification and solutions were prepared using a volumetric flask. The flask was placed on a MS6002S balance from Mettler Toledo with accuracy ±0.01 g and each component added to the flask was weighed. The flask was made to volume with deionised water. As mass and volume were accounted for simultaneously, the molarity of the solution and the mass fraction of each component in the solution were calculated without involving density data.

2.2. Methods

2.2.1. Vapour-liquid equilibrium (VLE) experiments

VLE of aqueous amine solutions was measured using four different experimental set-ups.

2.2.1.1. Modified Swietoslawaski ebulliometer. Vapour pressure of pure amines and VLE of binary amine/H_2O systems were measured using a modified Swietoslawski ebulliometer. The apparatus and the experimental procedure were the same as described by Kim et al. [36]. The pressure was measured and controlled by a DPI520 rack mounted pressure controller provided by Druck, and temperatures were measured by Pt-100 thermosensors (uncertainty of ±0.1 K).

When the vapour pressure of pure amines was measured (*P-T* data), the experiment started at low pressures to measure low boiling temperatures and then the pressure was gradually increased to generate data at higher temperatures. The binary VLE (*P-T-x-y* data) were measured at T = (353, 363 and 373) K starting with an 80 wt% aqueous amine solution. When stability was reached in temperature and pressure, a sample from the liquid phase and the vapour condensate was collected for amine analyses. A new experimental point was obtained after diluting the solution with deionised water.

The pure components vapour pressure was fitted to the Antoine equation, and along with the measured *P-T*-x-y data, the data were used to calculate the activity coefficient of each component i (c_i^{Exp}) in the liquid phase. The equation for the activity coefficient is given below [37]:

$$c_i^{Exp} = \frac{y_i P}{x_i P_i^{sat}} \cdot U_i \qquad (4)$$

where y_i and x_i, are the mole fraction of component i in the vapour and liquid phase, respectively, P is the total pressure and P_i^{sat} is the saturation pressure component i. The factor U_i, given in Eq. (5), was neglected as it is of negligible importance at low and moderate pressures.

$$U_i = \frac{\hat{U}_i}{U_i^{sat}} \exp\left(\frac{V^l (P - P^{sat})}{RT}\right) \qquad (5)$$

2.2.1.2. Low-pressure VLE apparatus. Vapour-liquid equilibrium (VLE) of CO_2 loaded amine systems in the temperature range of 313–353 K and at atmospheric pressure was measured using the low-pressure VLE apparatus applied in Ma'mun et al. [38] (see Fig 3). The apparatus consists of four glass cells with volume 360 cm^3, BÜHLER gas circulation pump and Rosemount X-stream CO_2 gas analyser equipped with two channels for CO_2 (0–1 ± 0.1% of full scale and 0–100 ±0.5% of full scale). The cells were immersed in a water bath and placed in a heating cabinet. The temperature of the water bath, the aqueous solution and the gas phase were recorded with K-type thermocouples with an uncertainty of T = ±0.1 K.

For each equilibrium measurement, around 150 mL pre-loaded amine solution was placed in cell two, three and four and flushed with N_2. Then, the gas phase was circulated through the liquid phase and the system was left to reach the experimental temperature. When constant temperature was reached, a bleed of the gas phase was cooled to temperatures between T = (283 and 288) K and the gas phase, now containing N_2, CO_2 and small amounts of H_2O and amine, was analysed for CO_2 content in the CO_2 analyser before the it was returned to the circulation loop. The system was assumed to be in equilibrium when a stable CO_2 gas phase composition was established. At equilibrium, a liquid sample of around 10 mL was collected from cell four for CO_2 and amine analysis. The remaining solution in the three cells was removed and diluted with pure amine solution or loaded with more CO_2 to obtain a new CO_2 loading. The amine solution was vigorously mixed and brought back to the three cells for a new equilibrium measurement.

The partial pressure of CO_2 was calculated as given in Eq. (6) where P_{CO_2} is the partial pressure of CO_2 at equilibrium, y_{CO_2} is

Table 1
Chemicals used in this work.

Chemical	CAS	Molar mass/(g mol^{-1})	Mass fraction purity as stated by supplier	Supplier
Monoethanolamine (MEA)	141-43-5	61.08	0.98	Sigma-Aldrich
3-(methylamino)propylamine (MAPA)	6291-84-5	88.15	0.97	Sigma-Aldrich
3-dimethylamino-1-propanol (3DMA1P)	3179-63-3	103.16	0.99	Acros organics
3-diethylamino-1-propanol (3DEA1P)	622-93-5	131.22	>0.95	TCI
1-(2-hydroxyethyl)pyrrolidine (1-(2HE)PRLD)	2955-88-6	115.17	0.97	Alfa Aesar
Carbon dioxide (CO_2)	124-38-9	44.01	0.99999	AGA
Nitrogen (N_2)	7727-37-9	28.01	0.99998	AGA

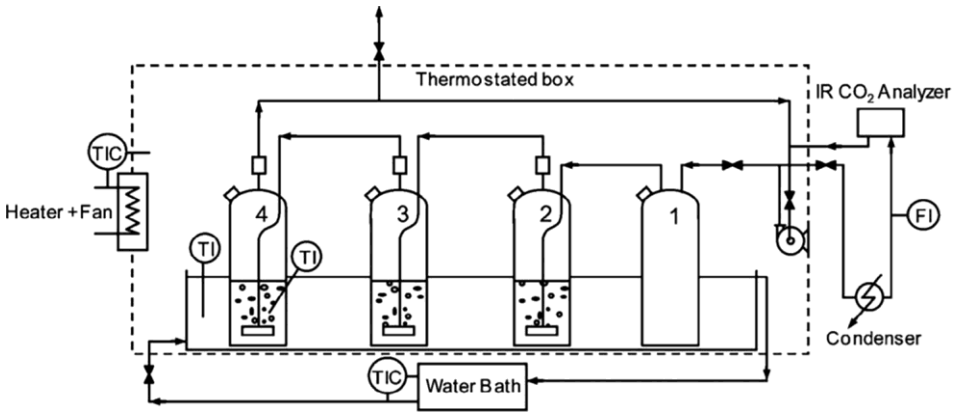

Fig.3. Schematic diagram of the low-pressure VLE apparatus [38].

the CO_2 concentration measured by the CO_2 analyser, P_{tot} is the total pressure, $P^{T^{exp}}_{solution}$ is the solvents vapour pressure at the equilibrium temperature and $P^{T_{condenser}}_{solution}$ is the vapour pressure of the solvent at the condenser temperature.

$$P_{CO_2} = y_{CO_2} P_{tot} - P^{T^{exp}}_{solution} - P^{T_{condenser}}_{solution} \quad (6)$$

The solvents vapour pressure at a given temperature was calculated by combining Dalton's law with Raoult's law. The vapour pressure of the pure component was calculated from the Riedel or Antoine's equation using parameters in Table 5.

2.2.1.3. High-pressure VLE apparatus. High-pressure VLE experiments for the CO_2 loaded amine systems were performed using two different VLE apparatus. The apparatuses were calorimeter CPA202 from Syrris (ChemiSens) described by Evjen et al. [39], hereafter referred to as VLE-1, and the medium-pressure VLE apparatus described by Hartono et al. [35], hereafter referred to as VLE-2. They were operated similarly, but the difference was the reactor volume (VLE-1: 0.3 L and VLE-2: 1.03 L) and that VLE-1 could be operated automatically with a procedure made in ProFind™. The reactor pressure in VLE-1 was measured with an uncertainty of ±1.5 kPa (10 bar max) and the reactor pressure in VLE-2 was measured with an uncertainty of ±0.2 kPa (2 bar and 6 bar max).

Only a brief description of VLE-1, illustrated in Fig. 4, is given here: The reactor was evacuated, charged with around 0.13 L amine solution and then once again evacuated. Under stirring at 400 rpm, the system was heated to the experimental temperature and left to equilibrate. At stable temperature, pressure and heat flow, CO_2 was injected from the CO_2 storage tank to the reactor. The system was again left to equilibrate before a new portion of CO_2 was injected into the reactor. This routine was repeated until the pressure in the reactor reached around 6 bar. At the end of the experiment, a liquid sample was collected for CO_2 and amine analysis. The partial pressure of CO_2 was calculated by subtracting the initial pressure from the total pressure (Eq. (7)). The initial pressure in the reactor was the pressure before the injection of CO_2. The amount of CO_2 added from the CO_2 storage tank to the reactor and the amount of CO_2 present in the gas phase of the reactor was calculated using the Peng-Robinson equation of state [40]. Then, the amount of CO_2 absorbed into the solution was obtained by a mass balance. The difference between this calculation method and the CO_2 loading determined from the CO_2 analysis was on average 2%.

$$P_{CO_2} = P_{tot} - P_{initial} \quad (7)$$

2.2.2. Analysis of liquid samples

Collected liquid samples were analysed for amine and CO_2 concentration. Amine concentration was determined by titrating a diluted liquid sample with 0.05 mol/dm³ H_2SO_4 using Mettler Toledo G20 compact titrator [38], while the CO_2 concentration was determined by total inorganic carbon (TIC) analysis using TOC-L provided by Shimadzu. During the TIC analysis, the liquid samples, diluted with a factor of 100, were injected and acidified in a 25 wt% H_3PO_4 solution. CO_2 and dissolved CO_2 were volatilised by a carrier gas sparged into the sample and detected with a non-dispersive infrared (NDIR) sensor.

2.2.3. NMR spectroscopy

Liquid samples collected from the low-pressure VLE apparatus were examined by means of NMR spectroscopy to characterise

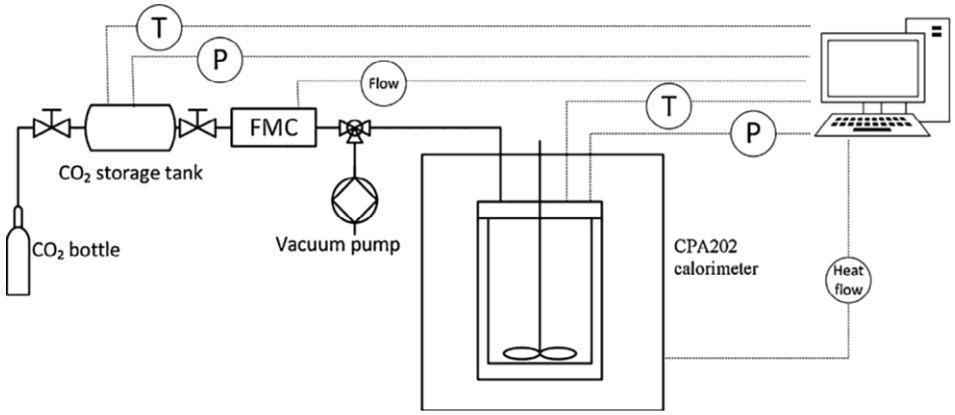

Fig. 4. Schematic diagram of VLE-1 (calorimeter CPA202) [39].

the species at equilibrium. In particular, the species concentrations were measured by acquiring quantitative ^{13}C NMR experiments at T = 300.0 K on a Bruker 600 MHz Avance III HD instrument equipped with a 5-mm cryogenic CP-TCI z-gradient probe, using the same method as described in Perinu et al. [41].

2.2.4. Activity coefficient models

Experimental binary VLE data were represented by a model coded in Matlab and an Aspen Plus model. ASPEN is a powerful simulation software widely used in the industry. It is used to design equipment and predict the performance of the chemical absorption process.

The two models applied the NRTL-model to calculate activity coefficients [42] and the Peng-Robinson equation of state to account for the systems vapour phase nonideality. The fitting of molecule-molecule binary interactions from the NRTL-model was performed in the model coded in Matlab. The energy parameters were temperature dependent as given in Eq. (8), and the non-randomness factor was fixed at 0.2. Parameters needed for the model are given in Table 2.

$$s_{ij} = a_{ij} + \frac{b_{ij}}{T/K} \quad (8)$$

For the Aspen Plus model, the fitted parameters for the Antoine equation and the fitted molecule-molecule binary interactions for the three tertiary amines studied in this work were implemented into Aspen Plus v9. The tertiary amines were already available in the Aspen Plus database, but the critical parameters were set as given in Table 2. The ideal gas heat capacity for 1-(2HE)PRLD was set equal to that of 3DEA1P.

2.2.5. Fitting of VLE data

VLE data for the CO_2 loaded amine blends were fitted to a parametrised function (Eq. (9)) proposed by Brúder et al. [8]. The function relates the CO_2 partial pressure to temperature and CO_2 loading but has no thermodynamic significance.

$$\ln\left(P_{CO_2}/\mathrm{kPa}\right) = A\ln\alpha + k_1 + \frac{B}{1 + k_2\exp(k_3\ln\alpha)} \quad (9)$$

Table 2
Density (ρ), molar volume (V_m), critical temperature (T_c) and pressure (P_c), and acentric factor (ω) for 3DMA1P, 3DEA1P and 1-(2HE)PRLD.

	3DMA1P	3DEA1P	1-(2HE)PRLD
ρ/(g cm^{-3})	0.8816 [43]	0.8600 [44]	0.9785 [45]
V_m/(m^3 kmol^{-1})	0.1170	0.1526	0.1177
T_c/K	626.41 [46]	716 [46]	666[a]
P_c/kPa	3790 [46]	3300 [46]	4104.535[a]
ω	0.841[a]	0.7316[a]	0.55061[a]

[a] Aspen Plus databank.

Table 3
Experimental equilibrium data for temperature T, and pressure P, for water, and the absolute relative deviation (ARD) from Riedel equation [47].[a]

T/K	P/kPa	% ARD
318.3	9.8	1.0
333.0	19.8	0.07
342.1	29.8	0.09
348.9	39.8	0.1
354.4	49.8	0.1
359.1	59.8	0.2
363.1	69.8	0.2
366.7	79.8	0.2
372.6	100.1	0.8

[a] Standard uncertainties u are $u(T)$ = 0.1 K and $u(P)$ = 0.8 kPa.

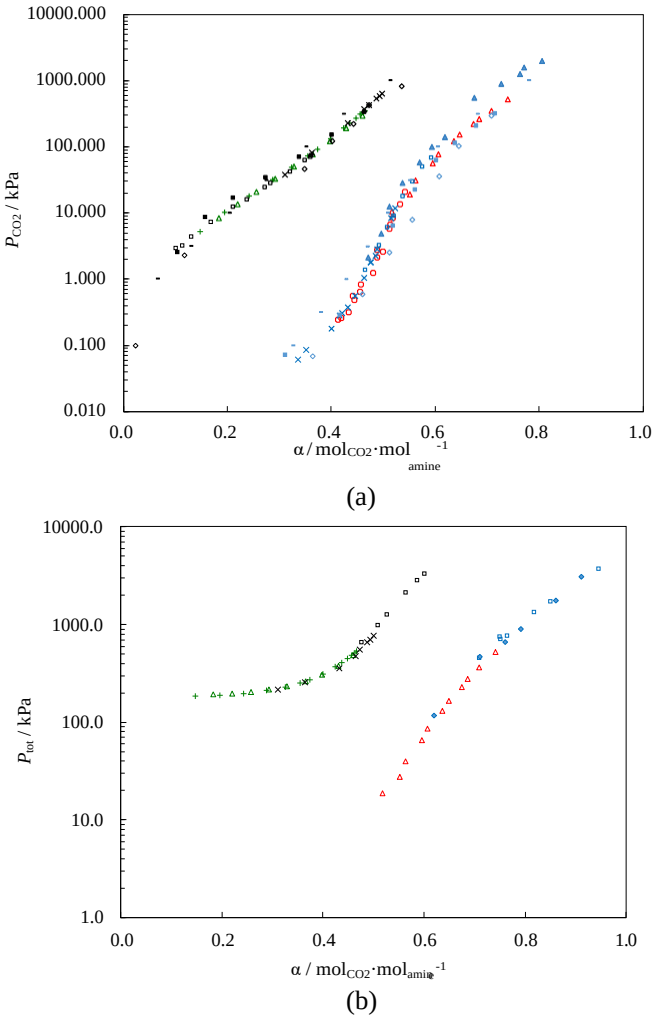

Fig. 5. CO_2 partial pressure (a) and total pressure (b) as a function of CO_2 loading (α) for the aqueous system 30 wt% MEA. Red, this work at T = 313 K; green, this work at T = 393 K; blue, literature data at T = 313 K; black, literature data at T = 393 K; (○) low-pressure VLE apparatus; (□) VLE-1; (+) VLE-2; (△) Aronu et al. [3]; (▽) Wagner et al. [51]; (◇) Jou et al. [49]; (–) Lee et al. [50]; (▯) Li et al. [53]; (▲) Shen and Li [48]; (▼) Kadiwala et al. [52]. (For interpretation of the references to colour in this figure legend, the reader is referred to the web version of this article.)

Table 4
Experimental equilibrium data for temperature T, and pressure P, for 3-dimethylamino-1-propanol (3DMA1P), 3-diethylamino-1-propanol (3DEA1P) and 1-(2-hydroxyethyl)pyrrolidine (1-(2HE)PRLD).[a]

T/K	P_{3DMA1P}/kPa	T/K	P_{3DEA1P}/kPa	T/K	$P_{1-(2HE)PRLD}$/kPa
352.3	4.8	353.9	1.8	360.6	2.8
352.9	4.8	360.2	2.8	372.2	4.8
368.3	9.8	405.3	19.8	388.8	9.8
378.5	14.8	409.2	22.3	405.5	19.8
378.5	14.8	412.1	24.8	417.0	29.8
385.8	19.8	420.2	34.8	426.1	39.8
396.8	29.8	427.3	44.8	432.6	49.8
405.0	39.8	433.4	54.8	438.1	59.8
411.6	49.8	440.1	64.8	442.6	69.8
417.2	59.8	442.2	69.8	446.9	79.8
421.7	69.8			449.8	89.8
426.3	79.8				
429.9	89.8				
433.7	99.8				

[a] Standard uncertainties u are $u(T)$ = 0.1 K and $u(P)$ = 0.8 kPa.

Table 5
Parameters (A, B, C, D, E) for the Riedel and the Antoine equation.

	A	B	C	D	E	equation	AARD%	Refs.
H_2O	73.649	7258.2	7.3037	4.1653 10 6	2	Riedel[a]		[47]
MEA	4.29252	1408.873	116.093			Antoine[b]		[55]
MAPA	14.86	3530.43	67.82			Antoine[c]		[23]
3DMA1P	10.169	2065.352	34.122			Antoine[d]	0.4	This work
3DEA1P	9.131	1397.896	116.086			Antoine[d]	2.4	This work
1-(2HE)PRLD	10.955	2689.681	2.401			Antoine[d]	1.2	This work

[a] $\ln P^{sat}_i = Pa = A + \frac{B}{T=K} + C\ln(T=K) + D(T=K)^E$.
[b] $\log_{10} P^{sat} = \text{bar} = A - \frac{B}{C + T=K}$.
[c] $\ln P^{sat}_i = kPa = A - \frac{B}{C + T=K}$.
[d] $\log_{10} P^{sat} = Pa = A + \frac{B}{C + T=K}$.

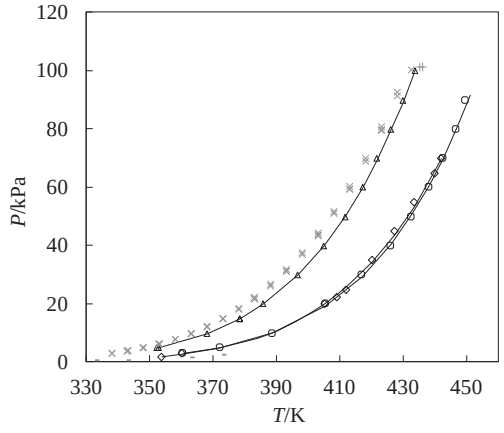

Fig. 6. Vapour pressure of alkanolamines as a function of temperature. (□) 3DMA1P, (○) 3DEA1P, (▽) 1-(2HE)PRLD, (–) 3DMA1P from Belabbaci et al. [33], (+) 3DMA1P from Kyrides et al. [54] and Kaluszyner and Galun [43], (△) DEEA from Hartono et al. [23] and (—) the Antoine equation.

2.2.6. Uncertainty analysis

To assess the uncertainty of the different apparatus, the combined standard uncertainty, u_c, was calculated (Tables 12–17). A generic calculation is given in Eqs. (10) and (11).

$$z = f(v_1; v_2; \ldots; v_n) \quad (10)$$

$$u_c(z) = \sqrt{\sum_{k=1}^{} \left(\frac{\partial f}{\partial v_k}\right)^2 u^2(v_k)} \quad (11)$$

Average absolute relative deviation (AARD) was calculated according to Eq. (12) where N is the number of experimental data points.

$$AARD = \% = \frac{100}{N} \sum_{1} \frac{Y_{calc} - Y_{Exp}}{Y_{Exp}} \quad (12)$$

3. Results and discussions

3.1. Validation of the experimental set-up

The experimental set-up and procedure of the ebulliometer were validated by measuring the boiling temperatures of water. With an AARD of only 0.3%, the data showed good agreement with the Riedel correlation for pure water given in Perry's Engineering Handbook [47] (Table 3). In addition, to estimate the hygroscopicity of 3DMA1P, 3DEA1P and 1-(2HE)PRLD, the amine concentration of each chemical in pure condition was analysed before and after a sample exposure to air for 8 hrs. Although this was an extreme case study, the change in amine concentration was found to be negligible (less than 1%). It was hence concluded that hygroscopicity would have a negligible effect on the reported properties obtained from the ebulliometer.

Table 6
Experimental (vapour + liquid) equilibrium data for temperature T, pressure P, liquid-phase mole fraction x with standard uncertainty $u(x_1)$ and vapour-phase mole fraction y with standard uncertainty $u(y_1)$, for the system 3-dimethylamino-1-propanol (1) + water (2).[a]

T/K	P/kPa	x_1	$u(x_1)$	y_1	$u(y_1)$
353.2	31.3	0.512	0.008	0.073	0.001
353.1	36.5	0.384	0.006	0.0509	0.0008
353.2	41.1	0.260	0.004	0.0343	0.0005
353.2	42.8	0.199	0.003	0.0289	0.0004
353.1	43.9	0.158	0.002	0.0242	0.0004
353.2	45.1	0.107	0.002	0.0197	0.0003
353.1	45.7	0.079	0.001	0.0159	0.0002
353.2	46.3	0.0526	0.0008	0.0133	0.0002
353.2	46.7	0.0354	0.0005	0.0106	0.0002
353.2	46.9	0.0237	0.0005	0.0078	0.0001
353.2	47.1	0.0166	0.0002	0.0062	0.00009
353.1	47.1	0.0118	0.0002	0.0045	0.00007
363.2	55.6	0.377	0.006	0.0524	0.0008
363.2	60.8	0.270	0.004	0.0388	0.0006
363.1	63.8	0.197	0.003	0.0302	0.0005
363.1	66.4	0.123	0.002	0.0238	0.0004
363.2	67.6	0.087	0.001	0.0192	0.0003
363.2	68.1	0.066	0.001	0.0170	0.0003
363.2	68.7	0.0503	0.0008	0.0147	0.0002
363.1	68.9	0.0397	0.0006	0.0128	0.0002
363.1	69.1	0.0313	0.0005	0.0112	0.0002
(1)					
373.1	72.7	0.474	0.007	0.073	0.001
373.1	89.4	0.272	0.004	0.0424	0.0006
373.2	95.1	0.171	0.003	0.0311	0.0005
373.2	97.1	0.117	0.002	0.0260	0.0004
373.2	97.9	0.097	0.001	0.0235	0.0004
373.2	98.6	0.080	0.001	0.0211	0.0003
373.2	99.1	0.067	0.001	0.0192	0.0003
373.2	99.6	0.0577	0.0009	0.0182	0.0003
373.2	99.8	0.0522	0.0008	0.0170	0.0003
(2)					
373.2	85.7	0.326	0.005	0.0483	0.0007
373.2	89.0	0.269	0.004	0.0427	0.0006
373.1	90.6	0.250	0.004	0.0403	0.0006
373.2	92.2	0.221	0.003	0.0363	0.0005
373.1	93.4	0.201	0.003	0.0335	0.0005
373.2	94.4	0.184	0.003	0.0321	0.0005
373.2	95.2	0.165	0.002	0.0300	0.0004
373.2	95.9	0.151	0.002	0.0287	0.0004
373.2	96.4	0.140	0.002	0.0279	0.0004
373.1	96.9	0.129	0.002	0.0265	0.0004
373.2	97.2	0.120	0.002	0.0259	0.0004
373.2	97.7	0.110	0.002	0.0245	0.0004
373.2	98.1	0.097	0.001	0.0233	0.0004

[a] Standard uncertainties u are $u(T)$ = 0.1 K and $u(P)$ = 0.8 kPa.

Table 7
Experimental (vapour + liquid) equilibrium data for temperature T, pressure P, liquid-phase mole fraction x with standard uncertainty $u(x_1)$ and vapour-phase mole fraction y with standard uncertainty $u(y_1)$, for the system 3-diethylamino-1-propanol (1) + water (2).[a]

T/K	P/kPa	x_1	$u(x_1)$	y_1	$u(y_1)$
(1)					
353.1	43.5	0.407	0.006	0.0197	0.0003
353.1	46.4	0.251	0.004	0.0169	0.0003
353.2	47.3	0.133	0.002	0.0160	0.0002
353.1	47.4	0.076	0.001	0.0153	0.0002
353.2	47.6	0.049	0.001	0.0151	0.0002
(2)					
352.8	19.5	0.78	0.01	0.0589	0.0009
353.2	26.0	0.72	0.01	0.0414	0.0006
353.2	31.0	0.64	0.01	0.0332	0.0005
353.2	33.3	0.597	0.009	0.0305	0.0005
353.2	38.2	0.529	0.008	0.0247	0.0004
353.2	40.9	0.517	0.008	0.0218	0.0003
353.2	42.5	0.427	0.006	0.0203	0.0003
353.1	44.7	0.338	0.005	0.0185	0.0003
(1)					
363.2	68.8	0.295	0.004	0.0197	0.0003
363.1	69.6	0.243	0.004	0.0188	0.0003
363.2	70.0	0.205	0.003	0.0186	0.0003
363.2	70.2	0.178	0.003	0.0184	0.0003
363.1	70.4	0.140	0.002	0.0180	0.0003
363.1	70.5	0.108	0.002	0.0177	0.0003
363.2	70.6	0.085	0.001	0.0177	0.0003
(2)					
363.2	55.8	0.567	0.009	0.0281	0.0004
363.1	60.9	0.479	0.007	0.0239	0.0004
363.2	64.3	0.412	0.006	0.0224	0.0003
363.2	65.4	0.382	0.006	0.0215	0.0003
363.2	66.4	0.358	0.005	0.0208	0.0003
363.2	67.1	0.332	0.005	0.0204	0.0003
363.2	68.0	0.296	0.004	0.0196	0.0003
363.1	68.7	0.263	0.004	0.0192	0.0003
(1)					
373.2	99.3	0.328	0.005	0.0226	0.0003
373.2	100.3	0.292	0.004	0.0219	0.0003
(2)					
373.1	51.9	0.72	0.01	0.0513	0.0008
373.3	63.3	0.67	0.01	0.0417	0.0006
373.1	72.6	0.610	0.009	0.0368	0.0006
373.2	79.3	0.547	0.008	0.0323	0.0005
373.2	90.3	0.484	0.007	0.0266	0.0004
373.2	96.4	0.375	0.006	0.0238	0.0004
373.1	99.6	0.295	0.004	0.0223	0.0003
373.2	99.6	0.294	0.004	0.0223	0.0003
373.2	100.7	0.250	0.004	0.0216	0.0003
373.2	101.3	0.229	0.003	0.0211	0.0003
373.2	101.9	0.194	0.003	0.0209	0.0003
373.2	101.9	0.170	0.003	0.0206	0.0003
373.1	102.0	0.131	0.002	0.0206	0.0003
373.2	102.2	0.103	0.002	0.0204	0.0003

[a] Standard uncertainties u are $u(T)$ = 0.1 K and $u(P)$ = 0.8 kPa.

Table 8
Experimental (vapour + liquid) equilibrium data for temperature T, pressure P, liquid-phase mole fraction x with standard uncertainty $u(x_1)$ and vapour-phase mole fraction y with standard uncertainty $u(y_1)$, for the system 1-(2-hydroxyethyl) pyrrolidine (1) + water (2).[a]

T/K	P/kPa	x_1	$u(x_1)$	y_1	$u(y_1)$
353.1	34.1	0.490	0.007	0.0229	0.0003
353.1	36.6	0.425	0.006	0.0197	0.0003
353.2	39.9	0.350	0.005	0.0166	0.0002
353.2	41.0	0.311	0.005	0.0146	0.0002
353.2	42.1	0.272	0.004	0.0139	0.0002
353.2	43.1	0.243	0.004	0.0127	0.0002
353.2	43.8	0.209	0.003	0.0113	0.0002
353.2	44.6	0.171	0.003	0.0109	0.0002
353.2	45.2	0.135	0.002	0.0097	0.0001
353.2	45.6	0.111	0.002	0.0090	0.0001
353.2	46.1	0.076	0.001	0.0084	0.0001
353.2	46.3	0.0615	0.0009	0.0078	0.0001
363.2	60.0	0.362	0.005	0.0185	0.0003
363.1	62.2	0.299	0.004	0.0163	0.0002
363.1	63.8	0.256	0.004	0.0153	0.0002
363.2	64.4	0.242	0.004	0.0142	0.0002
363.2	65.1	0.223	0.003	0.0140	0.0002
363.2	65.6	0.205	0.003	0.0132	0.0002
363.2	66.0	0.188	0.003	0.0127	0.0002
363.2	66.3	0.175	0.003	0.0130	0.0002
363.2	66.8	0.161	0.002	0.0121	0.0002
363.2	67.0	0.147	0.002	0.0119	0.0002
363.1	67.3	0.132	0.002	0.0117	0.0002
363.1	67.7	0.111	0.002	0.0108	0.0002
373.2	87.9	0.346	0.005	0.0212	0.0003
373.2	90.1	0.306	0.005	0.0196	0.0003
373.2	91.5	0.283	0.004	0.0184	0.0003
373.2	92.9	0.262	0.004	0.0177	0.0003
373.2	93.8	0.239	0.004	0.0168	0.0003
373.2	94.4	0.221	0.003	0.0164	0.0002
373.2	95.3	0.203	0.003	0.0155	0.0002
373.2	96.2	0.185	0.003	0.0150	0.0002
373.2	96.8	0.167	0.003	0.0147	0.0002
373.2	97.4	0.149	0.002	0.0140	0.0002
373.2	98.0	0.122	0.002	0.0134	0.0002
373.2	98.6	0.099	0.001	0.0124	0.0002

[a] Standard uncertainties u are $u(T)$ = 0.1 K and $u(P)$ = 0.8 kPa.

The VLE apparatus for low and high pressures were validated by measuring vapour-liquid equilibrium of the aqueous system 30 wt % MEA at T = 313 K and T = 393 K (see Fig. 5 and Tables A.1–A.2). The data generated in this work was between the data from Shen and Li [48], Jou et al. [49] and Lee et al. [50], and were in good agreement with the data from Aronu et al. [3], Wagner et al. [51], Kadiwala et al. [52] and the data from Li et al. [53] at T = 313 K. The saturated vapour pressure for 30 wt% MEA at 40 C calculated from Raoult's law for use in the data treatment for the low-pressure VLE apparatus (Table A.1) was comparable to the literature value of 6.4 kPa given in Kim et al. [36], while the initial pressure measured at 40 C when using VLE-1 (Table A.2) was around 2 kPa higher. There was a good agreement between the data generated using the different VLE apparatus.

3.2. Vapour pressure of pure amines

The measured vapour pressure of pure amines, covering the temperature range of 352–450 K, is presented in Table 4 and Fig. 6. The data were fitted to the Antoine equation, and the obtained parameters are given in Table 5. For 3DMA1P and 1-(2HE)PRLD, the AARD between the experimental data and the Antoine equation was less than 1.2%, while for 3DEA1P it was 2.4%.

In Fig. 6 it can be seen that 3DEA1P and 1-(2HE)PRLD have similar vapour pressures and are less volatile than 3DMA1P, while the vapour pressure of 3DMA1P is only slightly lower than that of DEEA reported by Hartono et al. [23]. Compared to the literature, the measured temperature of T = 433.7 K at 99.8 kPa for 3DMA1P was close to the boiling temperature of T = (436–437) K at atmospheric pressure reported by Kyrides et al. [54] and Kaluszyner and Galun [43], while the values reported by Belabbaci et al. [33] was lower than reported in this work. Belabbaci et al. [33] reported values in the range of 0.007–2.3 kPa at temperatures between 283.15 K and 373.10 K. Furthermore, it is reasonable that the vapour pressure of 3DMA1P is higher than that of 3DEA1P. Attached to the nitrogen atom, 3DMA1P has two methyl groups while 3DEA1P instead has two ethyl groups.

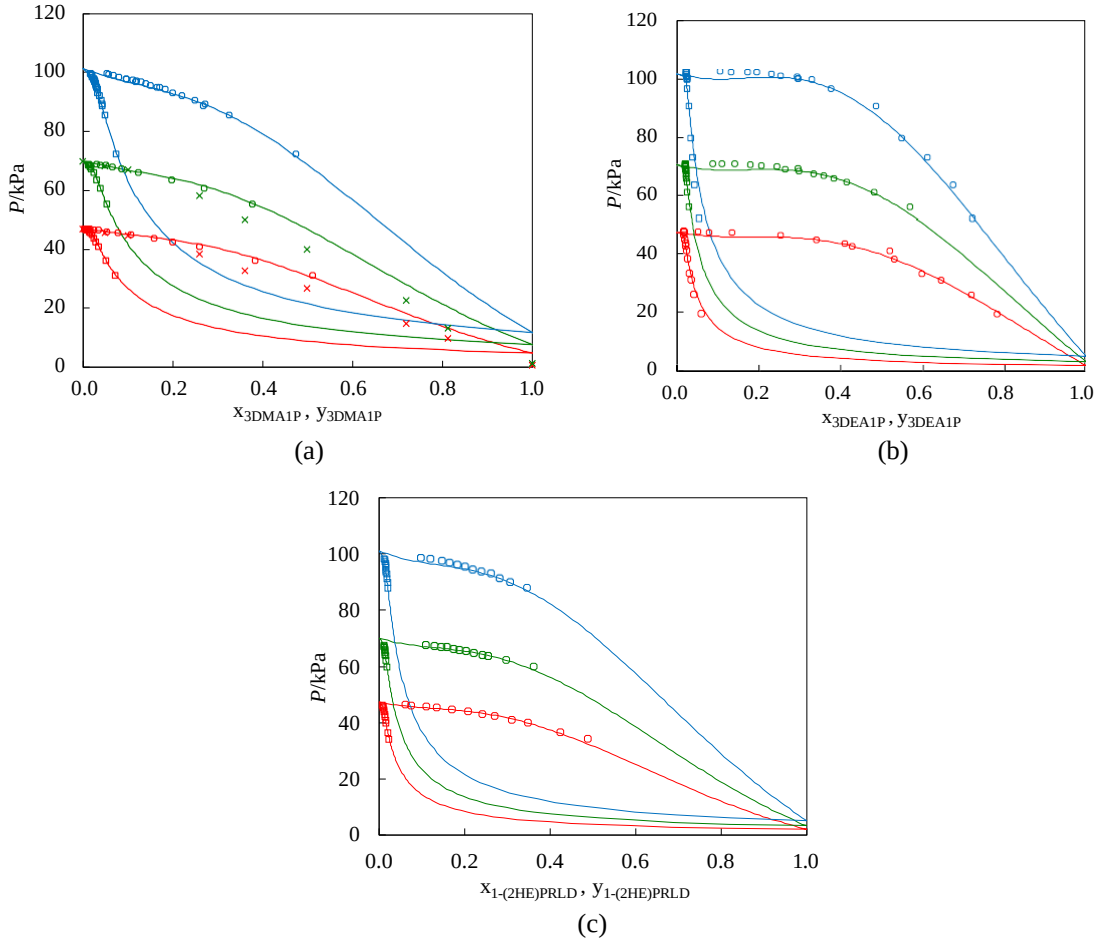

Fig. 7. Experimental and predicted binary VLE data for (a) 3DMA1P/H_2O, (b) 3DEA1P/H_2O and (c) 1-(2HE)PRLD/H_2O. Red, T = 353 K; green, T = 363 K; blue, T = 373 K; (s) liquid phase mole fraction; (h) vapour phase mole fraction, (—) NRTL model; ( ) Belabbaci et al. [33]. (For interpretation of the references to colour in this figure legend, the reader is referred to the web version of this article.)

Table 9
Parameter a and b for the NRTL-model.[a]

	3DMA1P (1) + H_2O (2)	3DEA1P (1) + H_2O (2)	1-(2HE)PRLD (1) + H_2O (2)
$a_{1,2}$	0.7274	11.3402	0.1156
$a_{2,1}$	0.0300	3.4824	1.1755
$b_{1,2}$	1233.0746	2504.3462	1715.8870
$b_{2,1}$	695.2484	785.4102	1103.8140

[a] $S_{1,2} = a_{1,2} + b_{1,2}/(T/K)$; $S_{2,1} = a_{2,1} + b_{2,1}/(T/K)$.

Table 10
AARD between the model and experimental data. In the table, P is pressure and y is vapour phase mole fraction.

	Number of data points	AARD (%)		
		P_{tot}	y_{H2O}	$y_{tertiary\ amine}$
3DMA1P/H_2O	43	0.8	0.1	2.4
3DEA1P/H_2O	44	1.6	0.2	6.5
1-(2HE)PRLD/H_2O	36	0.9	0.04	2.4

3.3. *Binary VLE of tertiary amine-H_2O systems*

The experimental P-T-x-y data for the three binary systems 3DMA1P/H_2O, 3DEA1P/H_2O and 1-(2HE)PRLD/H_2O are presented in Tables 6–8, respectively, and the data describes the composition of the liquid and vapour phase in equilibrium at a given total pressure and temperature. For instance, at T = 353.1 K and a total pressure of 47.1 kPa, the mole fraction of 3DMA1P in the liquid and the vapour phase was x = 0.0118 and y = 0.0045, respectively (Table 6).

Fig. 7 shows the P-x-y diagrams of the experimental data and the NRTL-model representing the VLE data. The regressed NRTL parameters are given in Table 9. Overall, the model represented P-T-x-y data well with AARD in the range of 0.1–6.5% (see Table 10). However, for all three systems, the models were slightly under predicting the experimental data at increasing temperature. Fig. 7a shows that the total pressure data for the binary 3DMA1P/H_2O system at T = 353 K and T = 363 K obtained in this work are slightly higher compared to the total pressures reported by Belabbaci et al. [33]. This was also the case for the vapour pressure of 3DMA1P (Section 3.2).

Further, the experimental and modelled activity coefficients for the binary systems are shown in Fig. 8. The activity coefficients showed low temperature dependency, and the three binary systems showed high non-ideality at low amine concentration.

To compare the volatility of the studied amines in the binary amine/H_2O systems, the modelled vapour phase mole fraction of the amines was plotted against the modelled liquid phase mole fraction at 80 C (Fig. 9). The NRTL-parameters for DEEA/H_2O were retrieved from Monteiro et al. [56]. Typically, the liquid mole fraction of amines in an aqueous amine solution varies from near zero to 0.2, and in this range the studied binary systems clearly showed a higher amine content in the vapour phase than MEA in the binary

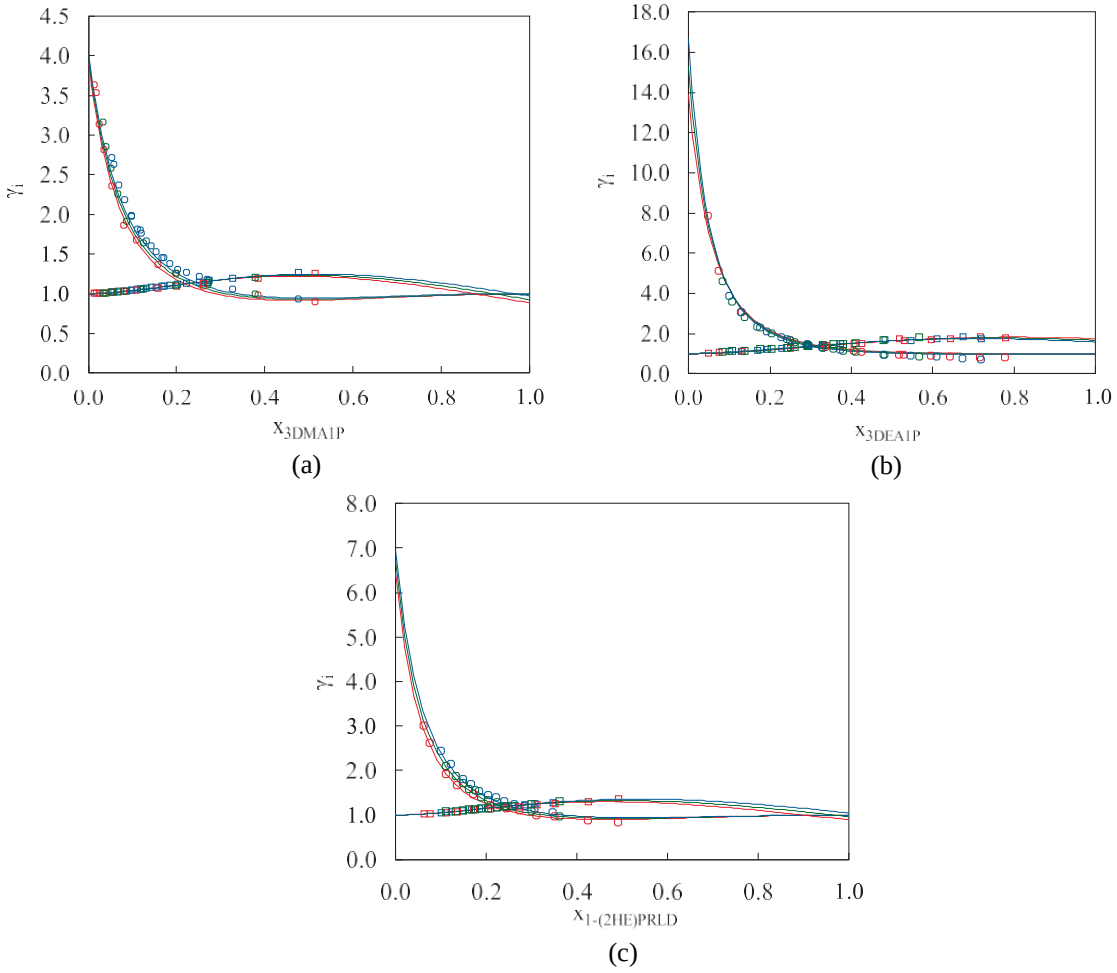

Fig. 8. Experimental and predicted activity coefficients (γ_i) for (a) 3DMA1P/H_2O, (b) 3DEA1P/H_2O and (c) 1-(2HE)PRLD/H_2O. (s) tertiary amine; (h) H_2O; red, T = 353 K; green, T = 363 K; blue, T = 373 K; (—) NRTL model. (For interpretation of the references to colour in this figure legend, the reader is referred to the web version of this article.)

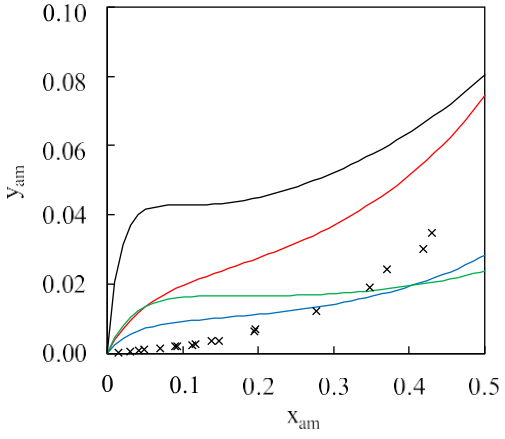

Fig. 9. x-y diagram for the binary amine/H_2O systems at T = 353 K. Black, DEEA/H_2O; red, 3DMA1P/H_2O; green, 3DEA1P/H_2O; blue, 1-(2HE)PRLD/H_2O; (x) MEA/H_2O [36]. (For interpretation of the references to colour in this figure legend, the reader is referred to the web version of this article.)

MEA/H_2O system [36]. This indicates that the tertiary amines were more volatile than MEA. Further, DEEA in the binary DEEA/H_2O system seemed to be more volatile than the other blended systems.

At an amine liquid mole fraction of 0.1, the vapour phase mole fraction of DEEA was twice as high as that of 3DMA1P and 3DEA1P and almost five times higher than that of 1-(2HE)PRLD. The solvents volatility is generally found to decrease with increasing CO_2 concentration, which in turn will reduce the volatility in a CO_2 capture process [57]. However, a water/acid wash section will be needed to eliminate amine loss through the exhaust gas.

Recently Du et al. [57] studied amine volatility in dilute amine/H_2O systems (<1.0 mol% amine) at 40 C and 1 atm, and developed a group contribution model that correlated Henry's law constant of amines (H_{am}) in water to their molecular structure. According to this model, the trend of increasing volatility of the amines was 1-(2HE)PRLD (812 Pa) < 3DMA1P (1790 Pa) < DEEA (3153 Pa) < 3DEA1P (4188 Pa). This is close to the trend seen from Fig. 9 at a liquid mole fraction of 0.01. The only difference is that, in this work, DEEA in the binary amine-water system seemed to be more volatile than 3DEA1P. The model by Du et al. [57] predicted a higher H_{am} value for 3DEA1P than DEEA due to the positive value assigned to the $-CH_2-$ group, which leads to higher H_{am} value when increasing the chain length.

As mentioned in Section 2.2.4, simulations were also performed in Aspen Plus v9 to predict the system's binary VLE behaviour (Figs. B.2 and B.3). A good prediction of P-T-x-y data in Aspen Plus is of high importance when the goal is to extend the Aspen Plus model to predict CO_2 VLE data. The model in Aspen Plus was able

Table 11
AARD between the Aspen Plus model and experimental data. In the table, P is pressure and y is vapour phase mole fraction.

	AARD (%)			
	Antoine equation for tertiary amine	P_{tot}	y_{H2O}	$y_{tertiary\ amine}$
3DMA1P/H_2O	2.0	0.6	0.1	3.3
3DEA1P/H_2O	11.9	1.7	1.2	43.8
1-(2HE)PRLD/H_2O	1.3	0.6	0.04	2.5

to represent the vapour pressure of 3DMA1P and 1-(2HE)PRLD and their binary VLE data with low AARD (see Table 11). However, the vapour pressure of 3DEA1P and the vapour mole fraction of 3DEA1P in the binary 3DEA1P/H_2O system were not well represented. Thus, the parameters obtained for 3DMA1P and 1-(2HE) PRLD systems can safely be implemented into Aspen Plus, while using the parameters given in Table 9 for 3DEA1P in Aspen Plus will not give as good fit as expected. This is most likely related to the bad fit of the Antoine equation as shown in Table 11.

Table 12
Experimental vapour-liquid equilibrium data for the aqueous system 3 mol/dm³ (w = 0.317) 3-dimethylamino-1-propanol + 1 mol/dm³ (w = 0.0903) 3-(methylamino) propylamine using the low-pressure VLE apparatus. In the table, T is temperature, P is pressure in which the partial pressure of CO_2 (P_{CO_2}) is with the combined standard uncertainty $u_c(P_{CO_2})$, y_{CO_2} is the CO_2 concentration in the gas phase measured by the analyser, a is the CO_2 loading with the standard uncertainity u(a) and w_{CO_2} is the mass fraction of CO_2 in the loaded solution with the standard uncertainity $u(w_{CO_2})$.[a]

T/K	P_{tot}/kPa	$P^{T_{exp}}_{solution}$/kPa	$P^{T_{condenser}}_{solution}$/k	a	y_{CO_2}	P_{CO_2}/kPa	$u_c(P_{CO_2})$/kPa	a/(mol$_{CO_2}$ mol$^{-1}_{amine}$)	u(a)/(mol$_{CO_2}$ mol$^{-1}_{amine}$)	w_{CO_2}	$u(w_{CO_2})$
(1)											
313.3	100.9	6.71	1.311		0.162	15.5	0.5	0.78	0.01	0.123	0.002
313.3	100.9	6.72	1.255		0.126	12.0	0.5	0.75	0.01	0.118	0.002
313.4	100.8	6.75	1.244		0.101	9.6	0.5	0.72	0.01	0.114	0.002
313.4	100.8	6.74	1.253		0.061	5.8	0.5	0.65	0.01	0.105	0.002
313.4	100.8	6.76	1.201		0.039	3.7	0.5	0.597	0.009	0.097	0.001
313.4	100.7	6.76	1.211		0.020	1.9	0.5	0.529	0.008	0.087	0.001
313.4	100.6	6.75	1.185		0.00763[b]	0.725	0.004	0.414	0.006	0.070	0.001
313.4	100.5	6.75	1.228		0.00242[b]	0.230	0.002	0.333	0.005	0.0565	0.0008
(2)											
313.4	100.5	6.74	1.231		0.190	18.0	0.5	0.79	0.01	0.125	0.002
313.4	100.5	6.76	1.216		0.104	9.9	0.5	0.72	0.01	0.115	0.002
313.4	100.6	6.75	1.233		0.057	5.4	0.5	0.65	0.01	0.105	0.002
313.4	100.6	6.75	1.186		0.00809[b]	0.769	0.004	0.415	0.006	0.070	0.001
313.4	100.6	6.76	1.145		0.00216[b]	0.205	0.001	0.325	0.005	0.0555	0.0008
333.1	100.0	17.93[c]	1.324		0.695	58.0	0.5	0.74	0.01	0.119	0.002
333.2	100.0	18.09[c]	1.334		0.488	40.6	0.5	0.72	0.01	0.116	0.002
333.4	100.0	18.23[c]	1.355		0.318	26.4	0.4	0.64	0.01	0.105	0.002
333.5	99.9	18.26[c]	1.327		0.207	17.1	0.4	0.602	0.009	0.099	0.001
333.4	99.9	18.22[c]	1.296		0.125	10.4	0.4	0.516	0.008	0.087	0.001
333.5	99.9	18.28[c]	1.275		0.073	6.1	0.4	0.461	0.007	0.078	0.001
333.4	99.9	18.26[c]	1.282		0.048	4.0	0.4	0.401	0.006	0.068	0.001
333.3	99.9	18.16[c]	1.275		0.032	2.7	0.4	0.383	0.006	0.066	0.001
333.4	99.8	18.18[c]	1.269		0.015	1.2	0.4	0.342	0.005	0.0592	0.0009
333.4	101.0	18.20[c]	1.321		0.00974[b]	0.819	0.005	0.296	0.004	0.0520	0.0008
333.3	101.1	18.16[c]	1.269		0.00800[b]	0.674	0.004	0.287	0.004	0.0506	0.0008
353.4	101.6	43.3[d]	1.088		0.806	47.9	0.5	0.532	0.008	0.089	0.001
353.3	101.6	43.2[d]	1.086		0.374	22.3	0.4	0.439	0.007	0.076	0.001
353.6	101.6	43.7[d]	1.109		0.158	9.3	0.3	0.353	0.005	0.0626	0.0009
353.7	101.6	43.8[d]	1.211		0.079	4.7	0.3	0.304	0.005	0.0536	0.0008
353.5	101.6	43.4[d]	1.168		0.074	4.4	0.3	0.297	0.004	0.0534	0.0008
353.4	101.1	43.2[d]	1.129		0.051	3.0	0.3	0.276	0.004	0.0492	0.0007
353.6	101.6	43.7[d]	1.230		0.038	2.2	0.3	0.256	0.004	0.0464	0.0007
353.0	101.6	42.5[d]	1.182		0.00480[b]	0.289	0.003	0.127	0.002	0.0228	0.0003

[a] The remaining part of the total pressure was N_2. Standard uncertainties u are $u(T)$ = 0.1 K, $u(P_{tot})$ = 0.5 kPa and $u(y_{CO_2})$ = 0.005. Combined standard uncertainties u_c are $u_c(w_{3DMA1P})$ = 0.004 and $u_c(w_{MAPA})$ = 0.005 for the solution prepared, respectvely, $u_c(P^{T_{exp}}_{solution})$ = 0.04 kPa and $u_c(P^{T_{condenser}}_{solution})$ = 0.008 kPa.
[b] Standard uncertainty u is $u(y_{CO_2}) = 1 \times 10^{-5}$.
[c] Combined standard uncertainty u_c is $u_c(P^{T_{exp}}_{solution})$ = 0.08 kPa.
[d] Combined standard uncertainty u_c is $u_c(P^{T_{exp}}_{solution})$ = 0.2 kPa.

Table 13
Experimental vapour-liquid equilibrium data for the aqueous system 3 mol/dm³ (w = 0.415) 3-diethylamino-1-propanol + 1 mol/dm³ (w = 0.0930) 3-(methylamino)propylamine using the low-pressure VLE apparatus. In the table, T is temperature, P is pressure, y_{CO_2} is the CO_2 concentration in the gas phase measured by the analyser, a is the CO_2 loading and w_{CO_2} is the mass fraction of CO_2 in the loaded solution.[a]

T/K	P_{tot}/kPa	$P^{T_{exp}}_{solution}$/kPa	$P^{T_{condenser}}_{solution}$/kPa	y_{CO_2}	P_{CO_2}/kPa	a/(mol$_{CO_2}$ mol^{-1})$_{amine}$	w_{CO_2}
313.2	100.8	6.47	1.110	0.314	30.0	0.89	0.138
313.3	100.8	6.52	1.090	0.1536	14.6	0.81	0.129
313.3	100.7	6.50	1.092	0.1212	11.5	0.79	0.125
313.3	100.7	6.52	1.073	0.0872	8.3	0.75	0.119
313.2	100.7	6.48	1.094	0.0710	6.8	0.71	0.114
313.2	100.7	6.48	1.089	0.0536	5.1	0.66	0.107
313.2	100.7	6.48	1.055	0.0414	3.9	0.62	0.101

[a] The remaining part of the total pressure was N_2. Standard uncertainties u are $u(T)$ = 0.1 K, $u(P_{tot})$ = 0.5 kPa, $u(y_{CO_2})$ = 0.005, u(a) = 0.01 mol$_{CO_2}$ mol^{-1} and $u(w_{CO_2})$ = 0.002. Combined uncertainties u_c are $u_c(w_{3DEA1P})$ = 0.01 and $u_c(w_{MAPA})$ = 0.007 for the solution prepared, respectvely, $u_c(P^{T_{exp}}_{solution})$ = 0.03 kPa, $u_c(P^{T_{condenser}}_{solution})$ = 0.007 kPa and $u_c(P_{CO_2})$ = 0.5 kPa.

Table 14
Experimental vapour-liquid equilibrium data for the aqueous system 3 mol/dm³ (w = 0.343) 1-(2-hydroxyethyl)pyrrolidine + 1 mol/dm³ (w = 0.0876) 3-(methylamino) propylamine using the low-pressure VLE apparatus. In the table, T is temperature, P is pressure in which the partial pressure of CO_2 (P_{CO_2}) is with the combined standard uncertainty $u_c(P_{CO_2})$, y_{CO_2} is the CO_2 concentration in the gas phase measured by the analyser, α is the CO_2 loading with the standard uncertainty $u(\alpha)$ and w_{CO_2} is the mass fraction of CO_2 in the loaded solution with the standard uncertainty $u(w_{CO_2})$.[a]

T/K	P_{tot}/kPa	$P^{T_{exp}}_{solution}$/kPa	$P^{T_{condenser}}_{solution}$/kPa	y_{CO_2}	P_{CO_2}/kPa	$u_c(P_{CO_2})$/kPa	α/(mol$_{CO_2}$ mol^{-1})$_{amine}$	$u(\alpha)$/(mol$_{CO_2}$ mol^{-1})$_{amine}$	w_{CO_2}	$u(w_{CO_2})$
(1)										
313.2	100.5	6.63	1.185	0.034	3.2	0.5	0.615	0.009	0.097	0.001
313.3	100.5	6.67	1.293	0.017	1.6	0.5	0.546	0.008	0.088	0.001
313.4	100.5	6.71	1.243	0.00355[b]	0.337	0.002	0.377	0.006	0.0622	0.0009
(2)										
313.3	100.6	6.68	1.247	0.043	4.1	0.5	0.64	0.01	0.102	0.002
313.1	100.3	6.59	1.357	0.015	1.4	0.5	0.587	0.009	0.093	0.001
313.4	100.2	6.70	1.288	0.01052[b]	0.998	0.005	0.475	0.007	0.078	0.001
313.4	100.2	6.71	1.241	0.00350[b]	0.331	0.002	0.378	0.006	0.0625	0.0009
313.5	100.1	6.74	1.255	0.00242[b]	0.229	0.002	0.355	0.005	0.0589	0.0009
(3)										
313.2	99.6	6.63	1.288	0.140	13.1	0.5	0.77	0.01	0.120	0.002
313.3	99.6	6.67	1.324	0.077	7.3	0.5	0.71	0.01	0.112	0.002
313.4	99.6	6.71	1.272	0.045	4.2	0.5	0.65	0.01	0.103	0.002
313.4	99.6	6.72	1.249	0.026	2.4	0.5	0.590	0.009	0.095	0.001
313.5	99.6	6.74	1.260	0.015	1.4	0.5	0.530	0.008	0.087	0.001
313.4	99.6	6.72	1.246	0.00802[b]	0.754	0.004	0.441	0.007	0.073	0.001
313.5	99.6	6.73	1.270	0.00343[b]	0.323	0.002	0.373	0.006	0.0621	0.0009
(1)										
333.3	99.6	18.04[c]	1.186	0.262	21.7	0.4	0.66	0.01	0.103	0.002
333.5	99.7	18.15[c]	1.246	0.156	12.9	0.4	0.584	0.009	0.093	0.001
333.5	99.7	18.18[c]	1.219	0.102	8.4	0.4	0.533	0.008	0.086	0.001
333.5	99.7	18.22[c]	1.195	0.082	6.8	0.4	0.500	0.008	0.081	0.001
333.4	99.7	18.11[c]	1.124	0.055	4.6	0.4	0.459	0.007	0.075	0.001
333.4	99.7	18.11[c]	1.134	0.024	2.0	0.4	0.400	0.006	0.067	0.001
333.4	99.8	18.11[c]	1.201	0.00652[b]	0.540	0.003	0.275	0.004	0.0464	0.0007
333.3	99.8	18.06[c]	1.192	0.00338[b]	0.280	0.002	0.234	0.004	0.0398	0.0006
(2)										
333.0	100.7	17.77[c]	1.181	0.508	42.7	0.5	0.75	0.01	0.118	0.002
333.3	100.7	18.01[c]	1.180	0.169	14.2	0.4	0.60	0.009	0.098	0.001
333.3	100.8	18.01[c]	1.211	0.072	6.0	0.4	0.49	0.007	0.081	0.001
333.4	100.8	18.11[c]	1.222	0.033	2.8	0.4	0.42	0.006	0.070	0.001
(3)										
333.2	99.5	17.95[c]	1.166	0.00615[b]	0.509	0.003	0.262	0.004	0.0459	0.0007
333.3	99.8	18.01[c]	1.200	0.00459[b]	0.381	0.002	0.271	0.004	0.0445	0.0007
352.9	101.4	42.1[d]	1.152	0.901	54.5	0.6	0.578	0.009	0.096	0.001
353.4	101.3	43.0[d]	1.139	0.564	33.5	0.4	0.502	0.008	0.085	0.001
353.3	101.3	42.7[d]	1.120	0.339	20.2	0.3	0.441	0.007	0.077	0.001
353.5	101.3	43.1[d]	1.115	0.187	11.1	0.3	0.383	0.006	0.068	0.001
353.2	101.3	42.7[d]	1.136	0.134	8.0	0.3	0.353	0.005	0.064	0.001
353.2	100.9	42.7[d]	1.191	0.071	4.2	0.3	0.310	0.005	0.054	0.001
353.4	100.3	42.9[d]	1.236	0.00850[b]	0.498	0.005	0.159	0.002	0.028	0.0004

[a] The remaining part of the total pressure was N_2. Standard uncertainties u are $u(T)$ = 0.1 K, $u(P_{tot})$ = 0.5 kPa and $u(y_{CO_2})$ = 0.005. Combined standard uncertainties u_c are $u_c(w_{1\text{-}(2HE)PRLD})$ = 0.009 and $u_c(w_{MAPA})$ = 0.006 for the solution prepared, respectively, $u_c(P^{T_{exp}}_{solution})$ = 0.04 kPa and $u_c(P^{T_{condenser}}_{solution})$ = 0.008 kPa.
[b] Standard uncertainty u is $u(y_{CO_2})$ = 1 10^{5}.
[c] Combined standard uncertainty u_c is $u_c(P_{solution})$ = 0.08 kPa.
[d] Combined standard uncertainty u_c is $u_c(P^{T_{exp}}_{solution})$ = 0.2 kPa.

3.4. Tertiary amine-MAPA-H_2O-CO_2 systems

Experimental VLE data for the tertiary amines blended with MAPA obtained from the low-pressure VLE apparatus are listed in Tables 12–14, and data obtained from the high-pressure VLE apparatus are given in Tables 15–17. The parameters obtained for the parameterised function (Eq. (9)) are listed in Table 18, and a comparison between the experimental data and the model is shown in Fig. 10. From the figure, it can be seen that there is a good agreement between the experimental data obtained using the different VLE apparatus and that there is a reasonably good agreement between the experimental data and the model. The obtained AARD for the tertiary amines 3DMA1P, 3DEA1P and 1-(2HE)PRLD blended with MAPA was 14.4%, 11.2% and 11.4%, respectively (Table 18). Thus, the developed model can then be further used to calculate the solvents heat of absorption of CO_2 through the Gibbs Helmholtz equation.

It should be noted that two phases were observed at low CO_2 loadings for the 3 mol/dm³ 3DEA1P + 1 mol/dm³ MAPA solution. Therefore, only a few equilibrium points were generated with the low-pressure VLE apparatus where the operation of systems forming two phases was difficult.

Further, the three solvent systems showed quite similar VLE behaviour and this is consistent with the NMR speciation data obtained for each amine system at increasing CO_2 loading (Fig. 11). Similarly to other MAPA-tertiary amine blends [41], the species identified and quantified at equilibrium were MAPA/MAPA(H^+)$_2$, primary MAPA carbamate (MAPA(H^+)$COO_{(p)}$), secondary MAPA carbamate (MAPA(H +)$COO_{(s)}$) and MAPA di-carbamate (MAPA$(COO)_2$), tertiary amine, tertiary amino carbonate and (bi)carbonate (HCO_3^-/CO_3^{2-}). In Fig. 11, it is observed that the MAPA-CO_2 derivative species and HCO_3^-/CO_3^{2-} follow a similar trend and are formed in comparable amounts, meaning that 3DMA1P, 1-(2HE)PRLD, 3DEA1P and DEEA affect MAPA reactions and CO_2 hydration similarly. These data are in

Table 15
Experimental vapour-liquid equilibrium data for the aqueous system 3 mol/dm³ (w = 0.317) 3-dimethylamino-1-propanol + 1 mol/dm³ (w = 0.0903) 3-(methylamino) propylamine using the apparatus VLE-1. In the table, T is temperature, P is pressure, α is the CO_2 loading and w_{CO_2} is the mass fraction of CO_2 in the loaded solution.[a]

T/K	P_{tot}/kPa	P_{CO_2}/kPa	α/(mol$_{CO_2}$ mol$^{-1}_{amine}$)	w_{CO_2}	T/K	P_{tot}/kPa	P_{CO_2}/kPa	α/(mol$_{CO_2}$ mol$^{-1}_{amine}$)	w_{CO_2}
313.1	9.5				373.2	99.3			
313.1	16.8	7.4	0.649	0.10490	373.1	111.9	12.6	0.257	0.04431
313.2	20.7	11.2	0.703	0.11267	373.1	133.3	34.0	0.341	0.05802
313.1	26.7	17.2	0.757	0.12026	373.1	171.8	72.5	0.424	0.07111
313.1	36.8	27.4	0.811	0.12767	373.1	229.6	130.3	0.505	0.08355
313.1	54.7	45.2	0.864	0.13495	373.2	312.3	213.0	0.584	0.09541
313.1	88.7	79.3	0.914	0.14166	373.1	431.1	331.8	0.661	0.10654
313.1	157.7	148.2	0.962	0.14791	373.1	605.3	506.0	0.733	0.11679
313.1	283.4	273.9	1.003	0.15330					
					393.1	193.6			
353.1	48.3				393.2	204.0	10.5	0.142	0.02493
353.2	57.3	9.0	0.351	0.05956	393.1	223.3	29.8	0.211	0.03672
353.1	69.8	21.5	0.438	0.07327	393.2	260.8	67.2	0.280	0.04813
353.1	90.1	41.8	0.524	0.08642	393.2	322.9	129.4	0.347	0.05889
353.1	121.8	73.5	0.610	0.09917	393.2	412.3	218.8	0.411	0.06903
353.1	172.6	124.2	0.693	0.11124	393.1	530.7	337.1	0.473	0.07870
353.2	260.1	211.7	0.774	0.12259					
353.1	419.6	371.3	0.848	0.13281					
353.1	692.9	644.6	0.912	0.14133					

[a] Standard uncertainties u are $u(T)$ = 0.1 K and $u(P_{tot})$ = 1.5 kPa. Combined standard uncertainites u_c *are* $u_c(w_{3DMA1P})$ = 0.004 and $u_c(w_{MAPA})$ = 0.005 for the solution prepared, respectvely, $u_c(P_{CO_2})$ = 2.1 kPa, $u_c(\alpha)$ = 0.005 mol$_{CO_2}$ mol$^{-1}_{amine}$ and $u_c(w_{CO_2})$ = 2×10^{-5}.

Table 16
Experimental vapour-liquid equilibrium data for the aqueous system 3 mol/dm³ (w = 0.415) 3-diethylamino-1-propanol + 1 mol/dm³ (w = 0.0930) 3-(methylamino)propylamine using the apparatus VLE-1. In the table, T is temperature, P is pressure, α is the CO_2 loading and w_{CO_2} is the mass fraction of CO_2 in the loaded solution.[a]

T/K	P_{tot}/kPa	P_{CO_2}/kPa	α/(mol$_{CO_2}$ mol$^{-1}_{amine}$)	w_{CO_2}	T/K	P_{tot}/kPa	P_{CO_2}/kPa	α/(mol$_{CO_2}$ mol$^{-1}_{amine}$)	w_{CO_2}
							(2)		
313.1	9.5				373.1	102.7			
313.2	18.2	8.8	0.735	0.11820	373.1	117.2	14.4	0.257	0.04556
313.2	28.1	18.6	0.826	0.13104	373.1	140.9	38.1	0.319	0.05596
313.2	61.6	52.1	0.916	0.14315	373.1	181.7	79.0	0.380	0.06588
313.1	180.5	171.0	0.984	0.15218	373.1	239.7	137.0	0.439	0.07545
					373.1	314.2	211.5	0.497	0.08457
(1)					373.1	403.8	301.0	0.554	0.09337
353.1	48.7				373.1	508.7	406.0	0.610	0.10182
353.1	56.6	8.0	0.319	0.05600					
353.1	70.8	22.1	0.398	0.06891			(1)		
353.1	93.6	44.9	0.476	0.08124	393.1	199.5			
353.2	124.3	75.6	0.553	0.09321	393.1	205.5	5.9	0.106	0.01926
353.1	163.2	114.5	0.630	0.10479	393.1	214.2	14.7	0.158	0.02853
353.1	211.1	162.4	0.706	0.11600	393.1	233.3	33.7	0.210	0.03749
353.1	271.1	222.4	0.781	0.12675	393.1	270.8	71.2	0.260	0.04608
353.2	394.0	345.3	0.851	0.13650	393.2	335.7	136.1	0.309	0.05423
353.1	624.3	575.6	0.910	0.14457	393.1	428.8	229.3	0.355	0.06182
					393.1	547.2	347.7	0.399	0.06898
(2)									
353.2	48.8						(2)		
353.1	65.2	16.7	0.373	0.06472	393.2	199.0			
353.1	85.0	36.5	0.445	0.07637	393.1	205.0	6.0	0.107	0.01947
353.1	112.9	64.5	0.518	0.08778	393.2	213.2	14.3	0.160	0.02886
353.2	148.1	99.7	0.590	0.09879	393.2	230.8	31.9	0.212	0.03795
353.1	191.1	142.7	0.662	0.10948	393.1	268.2	69.2	0.263	0.04659
353.1	243.1	194.7	0.733	0.11981	393.1	332.9	133.9	0.312	0.05475
353.1	314.9	266.5	0.802	0.12972	393.1	426.9	227.9	0.358	0.06233
					393.1	547.9	349.0	0.402	0.06952
(1)									
373.2	102.1								
373.1	107.3	5.1	0.207	0.03709					
373.1	121.5	19.4	0.275	0.04864					
373.1	154.6	52.4	0.342	0.05971					
373.1	209.8	107.7	0.407	0.07021					
373.1	284.4	182.3	0.470	0.08031					
373.1	377.7	275.6	0.532	0.08999					
373.2	489.7	387.5	0.593	0.09923					

[a] Standard uncertainties u are $u(T)$ = 0.1 K and $u(P_{tot})$ = 1.5 kPa. Combined standard uncertainites u_c *are* $u_c(w_{3DEA1P})$ = 0.01 and $u_c(w_{MAPA})$ = 0.007 for the solution prepared, respectvely, $u_c(P_{CO_2})$ = 2.1 kPa, $u_c(\alpha)$ = 0.005 mol$_{CO_2}$ mol$^{-1}_{amine}$ and $u_c(w_{CO_2})$ = 2×10^{-5}.

Table 17
Experimental vapour-liquid equilibrium data for the aqueous system 3 mol/dm³ (w = 0.344) 1-(2-hydroxyethyl)pyrrolidine + 1 mol/dm³ (w = 0.0876) 3-(methylamino) propylamine using the apparatuses VLE-1 and VLE-2. In the table, T is temperature, P is pressure, a is the CO_2 loading and w_{CO_2} is the mass fraction of CO_2 in the loaded solution.[a]

T/K	P_{tot}/kPa	P_{CO_2}/kPa	a/(mol$_{CO_2}$ mol^{-1})$_{amine}$	w_{CO_2}	T/K	P_{tot}/kPa	P_{CO_2}/kPa	a/(mol$_{CO_2}$ mol^{-1})$_{amine}$	w_{CO_2}
VLE-1					VLE-1 (2)				
313.2	8.7				373.2	99.4			
313.2	17.3	8.6	0.719	0.11169	373.1	105.4	6.0	0.227	0.03822
313.2	29.0	20.3	0.808	0.12383	373.1	112.2	12.7	0.283	0.04719
313.2	62.7	54.0	0.895	0.13538	373.1	123.7	24.3	0.339	0.05607
313.1	177.9	169.2	0.974	0.14562	373.1	141.1	41.7	0.395	0.06468
					373.1	165.2	65.8	0.450	0.07300
VLE-1					373.1	197.5	98.1	0.505	0.08114
353.2	46.2				373.1	239.6	140.1	0.558	0.08898
353.1	54.1	7.9	0.368	0.06044	373.1	294.8	195.3	0.611	0.09657
353.1	62.3	16.2	0.440	0.07146	373.1	367.1	267.6	0.662	0.10380
353.1	75.2	29.0	0.512	0.08229	373.1	463.0	363.6	0.711	0.11063
353.1	94.6	48.4	0.584	0.09273					
353.1	124.3	78.2	0.655	0.10284	VLE-1				
353.1	171.9	125.7	0.720	0.11194	393.1	194.2			
353.1	252.3	206.2	0.791	0.12162	393.1	206.6	12.4	0.172	0.02928
353.1	392.5	346.3	0.852	0.12977	393.1	222.5	28.2	0.229	0.03853
					393.1	247.9	53.7	0.285	0.04743
VLE-1 (1)					393.2	286.4	92.2	0.339	0.05605
373.1	98.7				393.1	338.5	144.3	0.393	0.06435
373.1	104.3	5.5	0.230	0.03876	393.1	407.2	212.9	0.445	0.07230
373.1	111.5	12.8	0.287	0.04789	393.1	492.8	298.5	0.496	0.07985
373.1	123.7	25.0	0.345	0.05687					
373.1	142.3	43.6	0.401	0.06556	VLE-2[b]				
373.1	168.0	69.3	0.457	0.07404	393.1	192.4			
373.1	201.6	102.9	0.511	0.08211	393.2	196.0	3.7	0.104	0.008868
373.1	245.0	146.3	0.565	0.08990	393.1	202.0	9.6	0.155	0.017841
373.1	302.4	203.7	0.617	0.09751	393.2	214.5	22.1	0.206	0.026449
373.2	376.8	278.1	0.669	0.10473	393.2	232.5	40.2	0.255	0.034744
373.1	475.8	377.1	0.717	0.11148	393.1	259.4	67.0	0.303	0.042773
					393.2	295.9	103.6	0.350	0.050406
					393.2	336.5	144.1	0.389	0.057646
					393.2	377.5	185.1	0.422	0.063735
					393.1	413.2	220.8	0.447	0.068748
					393.2	445.5	253.1	0.467	0.072492
					393.1	470.3	278.0	0.482	0.075584
					393.2	491.7	299.3	0.498	0.077763
					393.2	511.5	319.1	0.512	0.080146
					393.2	527.4	335.0	0.523	0.082263

[a] Standard uncertainties u are $u(T)$ = 0.1 K and $u(P_{tot})$ = 1.5 kPa. Combined standard uncertainites u_c are $u_c(w_{1\text{-(2HE)PRLD}})$ = 0.009 and $u_c(w_{MAPA})$ = 0.006 for the solution prepared, respectively, $u_c(P_{CO_2})$ = 2.1 kPa, u_c(a) = 0.005 mol$_{CO_2}$ mol$^{-1}_{amine}$ and $u_c(w_{CO_2})$ = 2 10^{-5}.

[b] Standard uncertainty u is $u(P_{tot})$ = 0.2 kPa. Combined standard uncertainties u_c are $u_c(P_{CO_2})$ = 0.3 kPa, u_c(a) = 4 10^{-4} mol$_{CO_2}$ mol^{-1} and $u_c(w_{CO_2})$ = 2 10^{-6}.

Table 18
Parameters for the CO_2 solubility correlation given in Eq. (9). In the table, T is temperature.

	3 mol/dm³ 3DMA1P + 1 mol/dm³ MAPA	3 mol/dm³ 3DEA1P + 1 mol/dm³ MAPA	3 mol/dm³ 1-(2HE)PRLD + 1 mol/dm³ MAPA
A	2.970	3.673	2.676
B	71.088	9.999	20.165
k_1	26:579ln T^{-1}=K 150:876	26:617ln T^{-1}=K 149:778	27:941ln T^{-1}=K 159:709
k_2	exp 1200:029 T^{-1}=K þ 6:738	exp 1212:067 T^{-1}=K þ 5:012	exp 1210:380 T^{-1}=K þ 5:264 k_3
	0:021 T^{-1}=K þ 2:855	55:012 T^{-1}=K þ 14:142	0:043 T^{-1}=K þ 2:165
AARD%	14.4	11.2	11.4

line with the findings reported in Bernhardsen et al. [26] and offer the possibility of using tertiary amines alternative to DEEA for the chemical absorption of CO_2 in the blend with MAPA.

Moreover, the three solvent systems obtained cyclic capacity above two on a mass basis (Table 19) in which 3DEA1P in the blend with MAPA obtained the highest with a value of 2.44 mol$_{CO_2}$ kg$^{-1}_{solution}$. The cyclic capacity was as in Section 1 calculated by considering absorption at T = 313 K and P_{CO_2} at 9.5 kPa, and desorption at T = 393 K and P_{CO_2} at 20.0 kPa (Eq. (3)). Compared to the solvents presented in Fig. 1, the obtained cyclic capacities were 66–95% higher than that of 30 wt% MEA and close to that of MAPA/2-dimethylaminoethanol (DMEA), MAPA/3-(diethylamino)-1,2-propanediol (DEA-1,2PD) and 2 mol/dm³ MAPA + 3 mol/dm³ DEEA.

4. Conclusions

This work studies the potential of using the tertiary amines 3DMA1P, 3DEA1P and 1-(HE)PRLD as an alternative to DEEA in the blend with MAPA. Vapour pressure of the three alkanolamines was measured in the temperature range of 352–450 K and VLE of the aqueous binary systems were measured at T = (353, 363 and 373) K. Antoine parameters were derived from vapour pressure data, and the NRTL-model was used to represent P-T-x-y data and activity coefficients. VLE of the CO_2 loaded tertiary amines blended with MAPA was measured in the temperature range T = 313 K to T = 393 K, and speciation data were obtained by NMR spectroscopy.

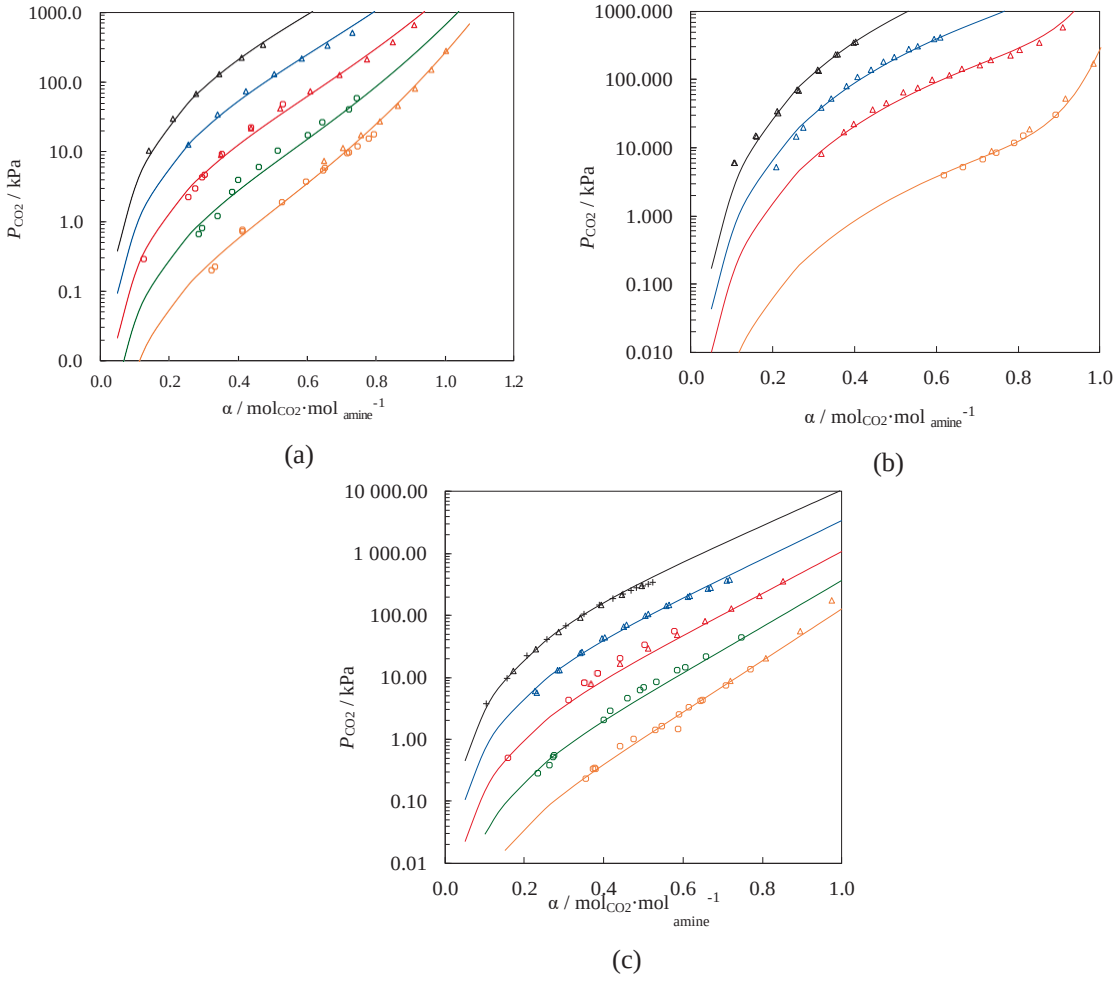

Fig. 10. Vapour-liquid equilibrium of (a) 3 mol/dm³ 3DMA1P + 1 mol/dm³ MAPA, (b) 3 mol/dm³ 3DEA1P + 1 mol/dm³ MAPA and (c) 3 mol/dm³ 1-(2HE)PRLD + 1 mol/dm³ MAPA. Orange, T = 313 K; green, T = 333 K; red, T = 353 K; blue, T = 373 K; black, T = 393 K; (s) low-pressure VLE apparatus; (□) VLE-1; (+) VLE-2. (For interpretation of the references to colour in this figure legend, the reader is referred to the web version of this article.)

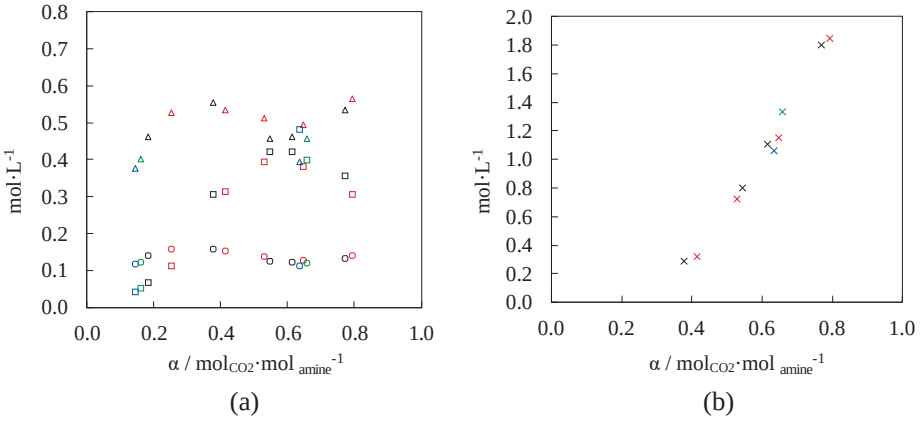

Fig. 11. Speciation data in blended MAPA solutions. (a) MAPA-CO_2 derivative species; (b) (bi)carbonate; red, 3 mol/dm³ 3DMA1P + 1 mol/dm³ MAPA; black, 3 mol/dm³ 1-(2HE)PRLD + 1 mol/dm³ MAPA; blue, 3 mol/dm³ 3DEA1P + 1 mol/dm³ MAPA reported in Perinu et al. [41]; green, 3 mol/dm³ DEEA + 1 mol/dm³ MAPA reported in Perinu et al. [41]; (□) MAPA(H^+)$COO_{(p)}$, (s) MAPA(H^+)$COO_{(s)}$; (h) MAPA$(COO)_2$; ( ) HCO_3^-/CO^2. (For interpretation of the references to colour in this figure legend, the reader is referred to the web version of this article.)

Based on the solvent's volatility and VLE behaviour, the tertiary amines investigated in this study can be used as an alternative to DEEA. In aqueous solution, 3DMA1P, 3DEA1P and 1-(2HE)PRLD were less volatile than DEEA. As a pure amine, 3DMA1P showed similar volatility as DEEA while 3DEA1P and 1-(2HE)PRLD were less volatile. Moreover, all three amines in the blend with MAPA obtained fairly similar VLE behaviour and obtained a cyclic capacity higher than 30 wt% MEA but comparable to other blended amines in the literature. The comparable VLE behaviour of the three blended amines was in line with the speciation data, indicating that the role of the current tertiary amines in the presence of MAPA was similar. The VLE data reported in this work can be used for rigorous process modelling.

Table 19
CO_2 cyclic capacity, Da, for blended amine solvents calculated from Eq. (3).

solution	Da/(mol$_{CO_2}$ mol$^{-1}_{amine}$)	Da/(mol$_{CO_2}$ kg$^{-1}_{solution}$)
3 mol/dm³ 3DMA1P + 1 mol/dm³ MAPA	0.51	2.09
3 mol/dm³ 3DEA1P + 1 mol/dm³ MAPA	0.58	2.44
3 mol/dm³ 1-(2HE)PRLD + 1 mol/dm³ MAPA	0.52	2.08

Acknowledgements

This work has been a part of the Low Energy Penalty Solvents (LEPS) project with grant number 243620/E20 under the CLIMIT programme. We gratefully acknowledge the Research Council of Norway for financial support.

Appendix A

Table A1
Experimental vapour-liquid equilibrium data for the aqueous system 30 wt% monoethanolamine using the low-pressure VLE apparatus. In the table, T is temperature, P is pressure in which the partial pressure of CO_2 (P_{CO_2}) is with the combined standard uncertainty $u_c(P_{CO_2})$, y_{CO_2} is the CO_2 concentration in the gas phase measured by the analyser, a is the CO_2 loading with the standard uncertainity u(a) and w_{CO_2} is the mass fraction of CO_2 in the loaded solution with the standard uncertainity $u(w_{CO_2})$. Data set A and B were generated with one year apart.[a]

T/K	P_{tot}/kPa	$P^{T_{solvent}^{exp}}$/kPa	$P^{T_{solvent}^{condenser}}$/kPa	y_{CO_2}	P_{CO_2}/kPa	$u_c(P_{CO_2})$/kPa	a/(mol$_{CO_2}$ mol$^{-1}_{amine}$)	u(a)/(mol$_{CO_2}$mol$^{-1}_{amine}$)	w_{CO_2}	$u(w_{CO_2})$
A(1)										
313.3	100.2	6.61	1.083	0.091	8.6	0.5	0.518	0.008	0.102	0.002
313.3	100.2	6.61	1.098	0.072	6.8	0.5	0.514	0.008	0.101	0.002
313.2	100.3	6.57	1.062	0.029	2.8	0.5	0.489	0.007	0.097	0.001
313.2	99.9	6.57	1.047	0.00914[b]	0.863	0.005	0.457	0.007	0.090	0.001
313.2	100.3	6.57	1.047	0.00606[b]	0.575	0.003	0.441	0.007	0.089	0.001
313.2	100.4	6.57	1.105	0.00269[b]	0.255	0.002	0.414	0.006	0.084	0.001
B(1)										
313.3	100.4	6.61	1.477	0.224	21.3	0.5	0.542	0.008	0.107	0.002
313.4	100.4	6.64	1.506	0.062	5.9	0.5	0.513	0.008	0.102	0.002
313.3	100.4	6.61	1.279	0.023	2.2	0.5	0.490	0.007	0.097	0.001
313.3	100.4	6.62	1.284	0.00688[b]	0.654	0.004	0.457	0.007	0.091	0.001
313.3	100.4	6.61	1.214	0.00345[b]	0.328	0.002	0.435	0.007	0.088	0.001
B(2)										
313.3	100.4	6.62	1.267	0.143	13.6	0.5	0.533	0.008	0.106	0.002
313.4	100.5	6.65	1.292	0.028	2.6	0.5	0.500	0.007	0.100	0.001
313.4	100.4	6.66	1.222	0.013	1.3	0.5	0.481	0.007	0.096	0.001
313.4	100.5	6.65	1.247	0.00526[b]	0.500	0.003	0.445	0.007	0.090	0.001
313.4	100.5	6.68	1.226	0.00281[b]	0.267	0.002	0.419	0.006	0.085	0.001

[a] The remaining part of the total pressure was N_2. Standard uncertainties u are $u(T)$ = 0.1 K, $u(P_{tot})$ = 0.5 kPa and $u(y_{CO_2})$ = 0.005. Combined uncertainties u_c are $u_c(w_{MEA})$ = 0.002 for the solution prepared, $u_c(P^{T_{solution}^{condenser}})$ = 0.008 kPa and $u_c(P^{T_{solution}^{exp}})$ = 0.04 kPa.

[b] Standard uncertainty u is $u(y_{CO_2}) = 1\ 10^{-5}$.

Appendix B

Table A2
Experimental vapour-liquid equilibrium data for the aqueous system 30 wt% monoethanolamine using the apparatuses VLE-1 and VLE-2. In the table, T is temperature, P is pressure, a is the CO_2 loading and w_{CO_2} is the mass fraction of CO_2 in the loaded solution.[a]

T/K	P_{tot}/kPa	P_{CO_2}/kPa	a/(mol$_{CO_2}$ mol^{-1})$_{amine}$	w_{CO_2}	T/K	P_{tot}/kPa	P_{CO_2}/kPa	a/(mol$_{CO_2}$ mol^{-1})$_{amine}$	w_{CO_2}
VLE-1 (1)					VLE-2[b]				
313.2	8.2				393.1	177.9			
313.2	18.8	10.5	0.518	0.09956	393.1	183.2	5.3	0.148	0.030809
313.2	39.4	31.2	0.563	0.10737	393.1	188.1	10.2	0.196	0.040509
313.2	85.5	77.3	0.607	0.11472	393.1	196.0	18.1	0.243	0.049758
313.2	162.9	154.7	0.648	0.12158	393.1	210.3	32.4	0.289	0.058533
313.1	274.1	265.9	0.686	0.12780	393.2	227.8	49.9	0.325	0.065342
					393.1	250.7	72.8	0.355	0.070982
VLE-1 (2)					393.2	271.2	93.3	0.374	0.074494
313.1	8.3				393.2	310.5	132.6	0.399	0.079212
313.1	27.5	19.2	0.552	0.10664	393.1	367.7	189.8	0.424	0.083749
313.2	64.7	56.4	0.595	0.11400	393.2	403.3	225.4	0.436	0.085870
313.2	130.3	122.0	0.636	0.12089	393.2	449.1	271.2	0.448	0.088072
313.1	227.9	219.6	0.674	0.12722	393.1	486.1	308.2	0.457	0.089566
313.2	359.5	351.2	0.709	0.13290	393.1	512.1	334.2	0.462	0.090499
313.2	524.6	516.3	0.741	0.13805	393.2	529.2	351.3	0.465	0.091067
VLE-1									
393.2	182.3								
393.1	190.8	8.5	0.183	0.03815					
393.1	195.9	13.6	0.220	0.04548					
393.1	203.5	21.2	0.257	0.05262					
393.1	215.0	32.7	0.293	0.05959					
393.1	232.6	50.3	0.329	0.06636					
393.1	259.8	77.5	0.365	0.07308					

(*continued on next page*)

Table A2 (*continued*)

T/K	P_{tot}/kPa	P_{CO_2}/kPa	α/(mol$_{CO_2}$ mol$^{-1}_{amine}$)	w_{CO_2}	T/K	P_{tot}/kPa	P_{CO_2}/kPa	α/(mol$_{CO_2}$ mol$^{-1}_{amine}$)	w_{CO_2}
393.1	303.6	121.4	0.398	0.07925					
393.1	372.4	190.1	0.430	0.08505					
393.1	478.2	296.0	0.460	0.09043					

[a] Standard uncertainties u are $u(T)$ = 0.1 K and $u(P_{tot})$ = 1.5 kPa. Combined standard uncertainites u_c *are* $u_c(w_{MEA})$ = 0.002 for the solution prepared, $u_c(P_{CO_2})$ = 2.1 kPa, $u_c(\alpha)$ = 0.005 mol$_{CO_2}$ mol$^{-1}_{amine}$ and $u_c(w_{CO_2})$ = 2 10^{-5}.

[b] Standard uncertainty u is $u(P_{tot})$ = 0.2 kPa. Combined standard uncertainties u_c are $u_c(P_{CO_2})$ = 0.3 kPa, $u_c(\alpha)$ = 4 10^{-4} mol$_{CO_2}$ mol^{-1} and $u_c(w_{CO_2})$ = 2 10^{-6}.

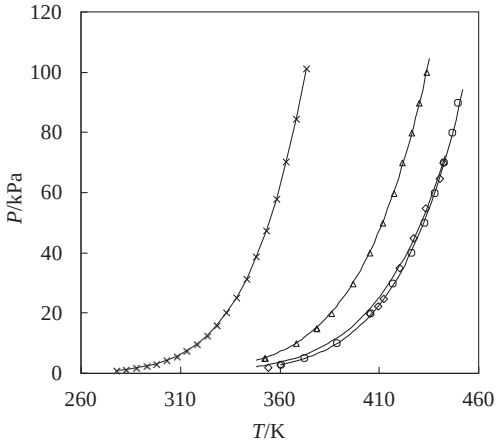

Fig. B1. Vapour pressure of pure alkanolamines ( ) H_2O from Riedel equation [47]; (D) 3DMA1P, (e) 3DEA1P; (s) 1-(2HE)PRLD; (—) Aspen Plus.

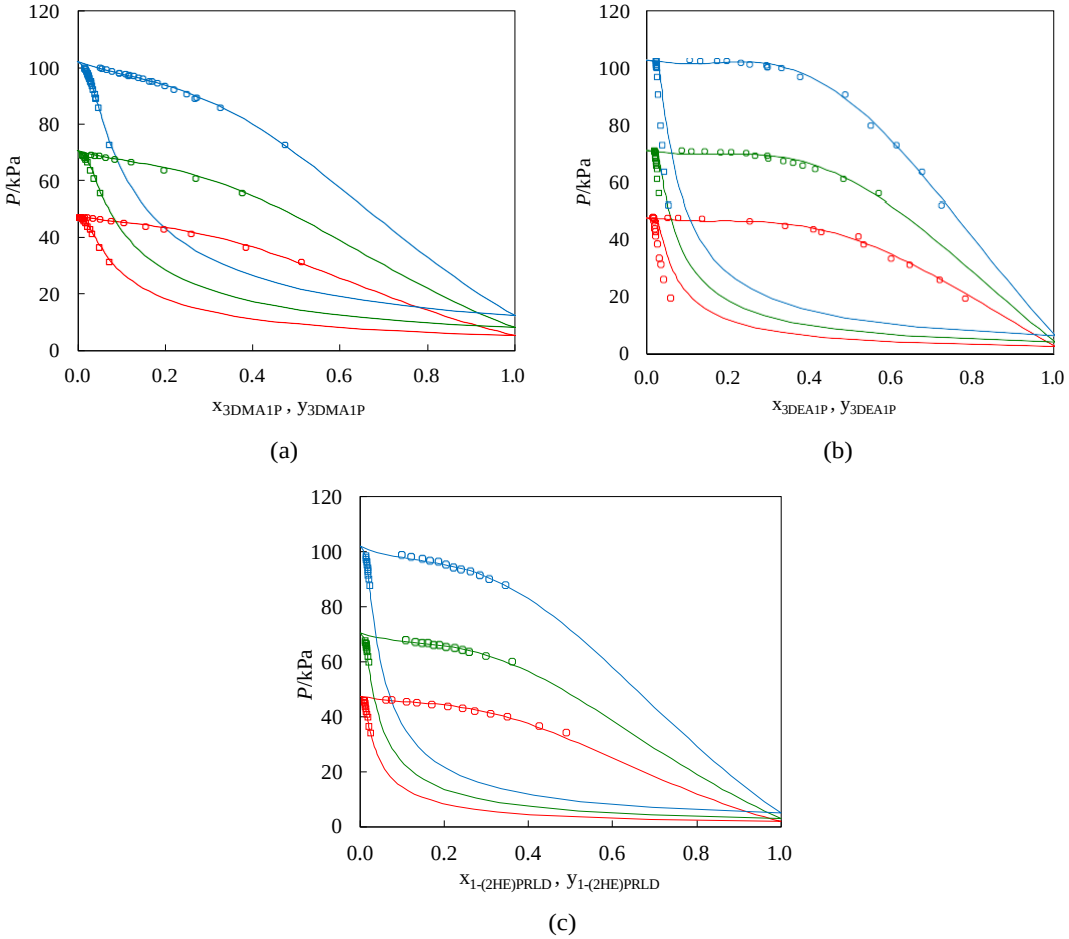

Fig. B2. Experimental and predicted binary VLE data for (a) 3DMA1P/H_2O, (b) 3DEA1P/H_2O and (c) 1-(2HE)PRLD/H_2O. Red, T = 353 K; green, T = 363 K; blue, T = 373 K; (s) liquid phase; (h) vapour phase, (—) Aspen Plus. (For interpretation of the references to colour in this figure legend, the reader is referred to the web version of this article.)

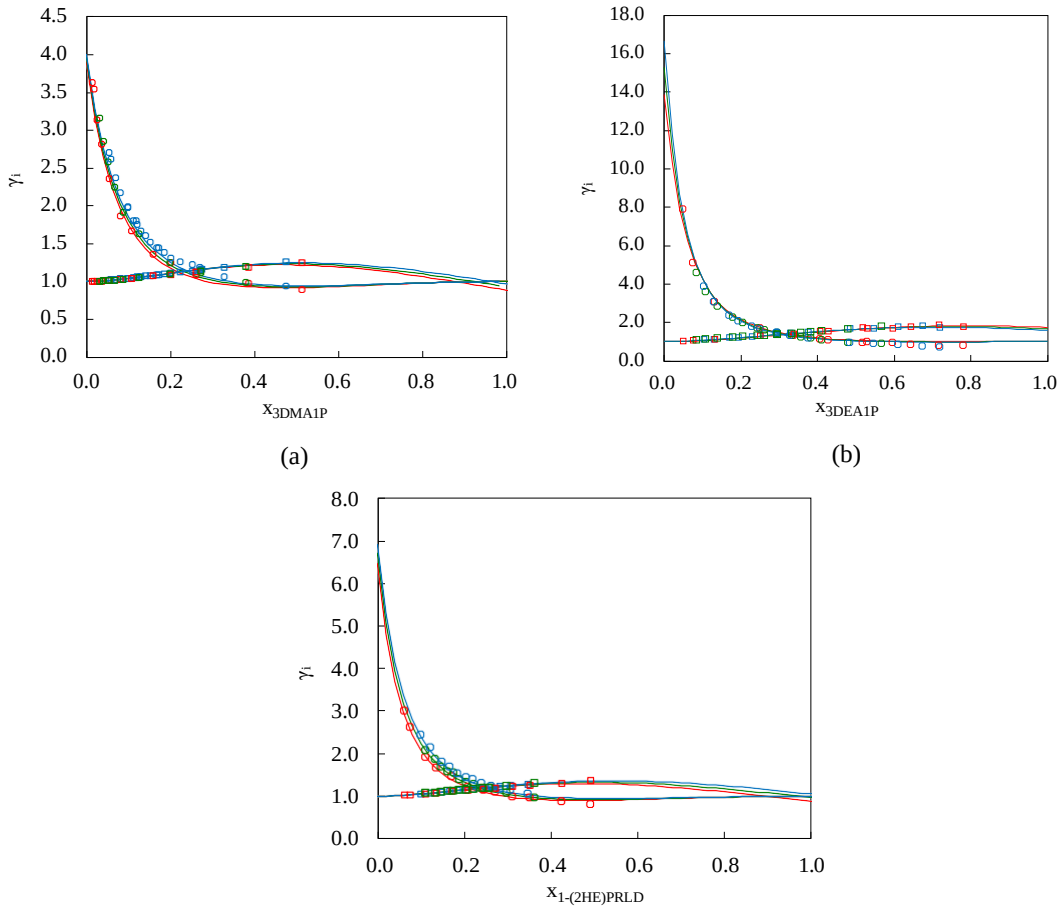

Fig. B3. Experimental and predicted activity coefficients (c_i) for (a) 3DMA1P/H_2O, (b) 3DEA1P/H_2O and (c) 1-(2HE)PRLD/H_2O. Red, T = 353 K; green, T = 363 K; blue, T = 373 K; (s) liquid phase; (h) vapour phase, (—) Aspen Plus. (For interpretation of the references to colour in this figure legend, the reader is referred to the web version of this article.)

Appendix C. Supplementary data

Supplementary data to this article can be found online at https://doi.org/10.1016/j.jct.2019.06.017.

References

[1] B. Walsh, P. Ciais, I.A. Janssens, J. Peñuelas, K. Riahi, F. Rydzak, D.P. van Vuuren, M. Obersteiner, Pathways for balancing CO2 emissions and sinks, Nat. Commun. 8 (2017) 14856, https://doi.org/10.1038/ncomms14856.

[2] Z. Liang, W. Rongwong, H. Liu, K. Fu, H. Gao, F. Cao, R. Zhang, T. Sema, A. Henni, K. Sumon, D. Nath, D. Gelowitz, W. Srisang, C. Saiwan, A. Benamor, M. Al-Marri, H. Shi, T. Supap, C. Chan, Q. Zhou, M. Abu-Zahra, M. Wilson, W. Olson, R. Idem, P. Tontiwachwuthikul, Recent progress and new developments in post-combustion carbon-capture technology with amine based solvents, Int. J. Greenhouse Gas Control 40 (2015) 26–54, https://doi.org/10.1016/j.ijggc.2015.06.017.

[3] U.E. Aronu, S. Gondal, E.T. Hessen, T. Haug-Warberg, A. Hartono, K.A. Hoff, H.F. Svendsen, Solubility of CO2 in 15, 30, 45 and 60 mass% MEA from 40 to 120 C and model representation using the extended UNIQUAC framework, Chem. Eng. Sci. 66 (2011) 6393–6406, https://doi.org/10.1016/j.ces.2011.08.042.

[4] F.-Y. Jou, F.D. Otto, A.E. Mather, Vapor-liquid equilibrium of carbon dioxide in aqueous mixtures of monoethanolamine and methyldiethanolamine, Ind. Eng. Chem. Res. 33 (1994) 2002–2005, https://doi.org/10.1021/ie00032a016.

[5] H.K. Knuutila, R. Rennemo, A.F. Ciftja, New solvent blends for post-combustion CO2 capture, Green Energy Environ. (2019), https://doi.org/10.1016/j.gee.2019.01.007, In press.

[6] M.W. Arshad, H.F. Svendsen, P.L. Fosbøl, N. von Solms, K. Thomsen, Equilibrium total pressure and CO2 solubility in binary and ternary aqueous solutions of 2-(diethylamino)ethanol (DEEA) and 3-(methylamino)propylamine (MAPA), J. Chem. Eng. Data 59 (2014) 764–774, https://doi.org/10.1021/je400886w.

[7] P. Brúder, K.G. Lauritsen, T. Mejdell, H.F. Svendsen, CO2 capture into aqueous solutions of 3-methylaminopropylamine activated dimethyl-monoethanolamine, Chem. Eng. Sci. 75 (2012) 28–37, https://doi.org/10.1016/j.ces.2012.03.005.

[8] P. Brúder, A. Grimstvedt, T. Mejdell, H.F. Svendsen, CO2 capture into aqueous solutions of piperazine activated 2-amino-2-methyl-1-propanol, Chem. Eng. Sci. 66 (2011) 6193–6198, https://doi.org/10.1016/j.ces.2011.08.051.

[9] D. Tong, G.C. Maitland, M.J.P. Trusler, P.S. Fennell, Solubility of carbon dioxide in aqueous blends of 2-amino-2-methyl-1-propanol and piperazine, Chem. Eng. Sci. 101 (2013) 851–864, https://doi.org/10.1016/j.ces.2013.05.034.

[10] H. Li, Y.L. Moullec, J. Lu, J. Chen, J.C.V. Marcos, G. Chen, Solubility and energy analysis for CO2 absorption in piperazine derivatives and their mixtures, Int. J. Greenhouse Gas Control 31 (2014) 25–32, https://doi.org/10.1016/j.ijggc.2014.09.012.

[11] S.J. Hwang, M. Lee, H. Kim, K.S. Lee, Cyclic CO2 absorption capacity of aqueous single and blended amine solvents, J. Ind. Eng. Chem. 65 (2018) 95–103, https://doi.org/10.1016/j.jiec.2018.04.017.

[12] H. Gao, B. Xu, H. Liu, Z. Liang, Effect of amine activators on aqueous N, N-diethylethanolamine solution for postcombustion CO2 capture, Energy Fuels 30 (2016) 7481–7488, https://doi.org/10.1021/acs.energyfuels.6b00671.

[13] S.K. Wai, C. Nwaoha, C. Saiwan, R. Idem, T. Supap, Absorption heat, solubility, absorption and desorption rates, cyclic capacity, heat duty, and absorption kinetic modeling of AMP–DETA blend for post–combustion CO2 capture, Sep. Purif. Technol. 194 (2018) 89–95, https://doi.org/10.1016/j.seppur.2017.11.024.

[14] D.-J. Seo, W.-H. Hong, Solubilities of carbon dioxide in aqueous mixtures of diethanolamine and 2-amino-2-methyl-1-propanol, J. Chem. Eng. Data 41 (1996) 258–260, https://doi.org/10.1021/je950197o.

[15] G. Kumar, M. Kundu, Vapor-liquid equilibrium of CO2 in aqueous blends of (N-ethyl-ethanolamine + N-Methyl-diethanolamine) and (N-ethyl-ethanolamine + 2-amino-2-methyl-1-propanol), J. Chem. Eng. Data 58 (2013) 2959–2965, https://doi.org/10.1021/je4004492.

[16] C. Guo, S. Chen, Y. Zhang, Solubility of carbon dioxide in aqueous 2-(2-aminoethylamine)ethanol (AEEA) solution and its mixtures with n-methyldiethanolamine/2-amino-2-methyl-1-propanol, J. Chem. Eng. Data 58 (2013) 460–466, https://doi.org/10.1021/je301174v.

[17] Y.-C. Chang, R.B. Leron, M.-H. Li, Equilibrium solubility of carbon dioxide in aqueous solutions of (diethylenetriamine + piperazine), J. Chem. Thermodyn. 64 (2013) 106–113, https://doi.org/10.1016/j.jct.2013.05.005.

[18] R. Ramazani, S. Mazinani, A. Hafizi, A. Jahanmiri, Equilibrium solubility of carbon dioxide in aqueous blend of monoethanolamine (MEA) and 2–1-

piperazinyl-ethylamine (PZEA) solutions: experimental and optimization study, Process Saf. Environ. Prot. 98 (2015) 325–332, https://doi.org/10.1016/j.psep.2015.09.003.
[19] D.D.D. Pinto, H. Knuutila, G. Fytianos, G. Haugen, T. Mejdell, H.F. Svendsen, CO2 post combustion capture with a phase change solvent. Pilot plant campaign, Int. J. Greenhouse Gas Control 31 (2014) 153–164, https://doi.org/10.1016/j.ijggc.2014.10.007.
[20] M.W. Arshad, P.L. Fosbøl, N. von Solms, H.F. Svendsen, K. Thomsen, Heat of absorption of CO2 in phase change solvents: 2-(diethylamino)ethanol and 3-(methylamino)propylamine, J. Chem. Eng. Data 58 (2013) 1974–1988, https://doi.org/10.1021/je400289v.
[21] H.K. Knuutila, Å. Nannestad, Effect of the concentration of MAPA on the heat of absorption of CO2 and on the cyclic capacity in DEEA-MAPA blends, Int. J. Greenhouse Gas Control 61 (2017) 94–103, https://doi.org/10.1016/j.ijggc.2017.03.026.
[22] J.G.M.S. Monteiro, H. Majeed, H. Knuutila, H.F. Svendsen, Kinetics of CO2 absorption in aqueous blends of N, N-diethylethanolamine (DEEA) and N-methyl-1,3-propane-diamine (MAPA), Chem. Eng. Sci. 129 (2015) 145–155, https://doi.org/10.1016/j.ces.2015.02.001.
[23] A. Hartono, F. Saleem, M.W. Arshad, M. Usman, H.F. Svendsen, Binary and ternary VLE of the 2-(diethylamino)-ethanol (DEEA)/3-(methylamino)-propylamine (MAPA)/water system, Chem. Eng. Sci. 101 (2013) 401–411, https://doi.org/10.1016/j.ces.2013.06.052.
[24] A.F. Ciftja, A. Hartono, H.F. Svendsen, Experimental study on phase change solvents in CO2 capture by NMR spectroscopy, Chem. Eng. Sci. 102 (2013) 378–386, https://doi.org/10.1016/j.ces.2013.08.036.
[25] J.G.M.S. Monteiro, S. Hussain, H. Majeed, E.O. Mba, A. Hartono, H. Knuutila, H.F. Svendsen, Kinetics of CO2 absorption by aqueous 3-(methylamino) propylamine solutions: experimental results and modeling, AIChE J. 60 (2014) 3792–3803, https://doi.org/10.1002/aic.14546.
[26] I.M. Bernhardsen, I.R.T. Krokvik, C. Perinu, D.D.D. Pinto, K.J. Jens, H.K. Knuutila, Influence of pKa on solvent performance of MAPA promoted tertiary amines, Int. J. Greenhouse Gas Control 68 (2018) 68–76, https://doi.org/10.1016/j.ijggc.2017.11.005.
[27] A. Nouacer, F.B. Belaribi, I. Mokbel, J. Jose, Solubility of carbon dioxide gas in some 2.5 M tertiary amine aqueous solutions, J. Mol. Liq. 190 (2014) 68–73, https://doi.org/10.1016/j.molliq.2013.10.026.
[28] M. Xiao, H. Liu, H. Gao, Z. Liang, CO2 absorption with aqueous tertiary amine solutions: equilibrium solubility and thermodynamic modeling, J. Chem. Thermodyn. 122 (2018) 170–182, https://doi.org/10.1016/j.jct.2018.03.020.
[29] A.V. Rayer, A. Henni, Heats of absorption of CO2 in aqueous solutions of tertiary amines: N-methyldiethanolamine, 3-dimethylamino-1-propanol, and 1-dimethylamino-2-propanol, Ind. Eng. Chem. Res. 53 (2014) 4953–4965, https://doi.org/10.1021/ie4041324.
[30] L. Rodier, K. Ballerat-Busserolles, J.-Y. Coxam, Enthalpy of absorption and limit of solubility of CO2 in aqueous solutions of 2-amino-2-hydroxymethyl-1,3-propanediol, 2-[2-(dimethyl-amino)ethoxy] ethanol, and 3-dimethyl-amino-1-propanol at T = (313.15 and 353.15) K and pressures up to 2 MPa, J. Chem. Thermodyn. 42 (2010) 773–780, https://doi.org/10.1016/j.jct.2010.01.015.
[31] S. Kadiwala, A.V. Rayer, A. Henni, Kinetics of carbon dioxide (CO2) with ethylenediamine, 3-amino-1-propanol in methanol and ethanol, and with 1-dimethylamino-2-propanol and 3-dimethylamino-1-propanol in water using stopped-flow technique, Chem. Eng. J. 179 (2012) 262–271, https://doi.org/10.1016/j.cej.2011.10.093.
[32] Z. Idris, J. Chen, D.A. Eimer, Densities of unloaded and CO2-loaded 3-dimethylamino-1-propanol at temperatures (293.15 to 343.15) K, J. Chem. Thermodyn. 97 (2016) 282–289, https://doi.org/10.1016/j.jct.2016.02.007.
[33] A. Belabbaci, N. Chiali-Baba Ahmed, I. Mokbel, L. Negadi, Investigation of the isothermal (vapour + liquid) equilibria of aqueous 2-amino-2-methyl-1-propanol (AMP), N-benzylethanolamine, or 3-dimethylamino-1-propanol solutions at several temperatures, J. Chem. Thermodyn. 42 (2010) 1158–1162, https://doi.org/10.1016/j.jct.2010.04.015.
[34] H. Liu, M. Li, R. Idem, P. Tontiwachwuthikul, Z. Liang, Analysis of solubility, absorption heat and kinetics of CO2 absorption into 1-(2-hydroxyethyl) pyrrolidine solvent, Chem. Eng. Sci. 162 (2017) 120–130, https://doi.org/10.1016/j.ces.2016.12.070.
[35] A. Hartono, R. Rennemo, M. Awais, S.J. Vevelstad, O.G. Brakstad, I. Kim, H.K. Knuutila, Characterization of 2-piperidineethanol and 1-(2-hydroxyethyl) pyrrolidine as strong bicarbonate forming solvents for CO2 capture, Int. J. Greenhouse Gas Control 63 (2017) 260–271, https://doi.org/10.1016/j.ijggc.2017.05.021.
[36] I. Kim, H.F. Svendsen, E. Børresen, Ebulliometric determination of vapor liquid equilibria for pure water, monoethanolamine, N-methyldiethanolamine, 3-(Methylamino)-propylamine, and their binary and ternary solutions, J. Chem. Eng. Data 53 (2008) 2521–2531, https://doi.org/10.1021/je800290k.
[37] H.C. Van Ness, Thermodynamics in the treatment of vapor/liquid equilibrium (VLE) data, Pure Appl. Chem. 67 (1995) 859, https://doi.org/10.1351/pac199567060859.
[38] S. Ma'mun, J.P. Jakobsen, H.F. Svendsen, O. Juliussen, Experimental and modeling study of the solubility of carbon dioxide in aqueous 30 Mass% 2- ((2-aminoethyl)amino)ethanol Solution, Ind. Eng. Chem. Res. 45 (2006) 2505–2512, https://doi.org/10.1021/ie0505209.
[39] S. Evjen, A. Fiksdahl, D.D.D. Pinto, H.K. Knuutila, New polyalkylated imidazoles tailored for carbon dioxide capture, Int. J. Greenhouse Gas Control 76 (2018) 167–174, https://doi.org/10.1016/j.ijggc.2018.06.017.
[40] D.-Y. Peng, D.B. Robinson, A new two-constant equation of state, Ind. Eng. Chem. Fundam. 15 (1976) 59–64, https://doi.org/10.1021/i160057a011.
[41] C. Perinu, I.M. Bernhardsen, D.D.D. Pinto, H.K. Knuutila, K.-J. Jens, NMR speciation of aqueous MAPA, tertiary amines, and their blends in the presence of CO2: influence of pKa and reaction mechanisms, Ind. Eng. Chem. Res. 57 (2018) 1337–1349, https://doi.org/10.1021/acs.iecr.7b03795.
[42] C.-C. Chen, L.B. Evans, A local composition model for the excess Gibbs energy of aqueous electrolyte systems, AIChE J. 32 (1986) 444–454, https://doi.org/10.1002/aic.690320311.
[43] A. Kaluszyner, A. Galun, Notes-N-methylation of amino alcohols and amino mercaptans, J. Organ. Chem. 26 (1961) 3536–3537, https://doi.org/10.1021/jo01067a619.
[44] K.N. Campbell, B.K. Campbell, The preparation of amino alcohols, Proc. Indiana Acad. Sci. 49 (1940) 101–104.
[45] A.L.K. Mndzhoyan, Amines and their derivatives. VIII. Synthesis of some symmetrical and unsymmetrical thioalkane di-, tri-, and tetraammonium compounds, Armyanskoi SSR, Khimicheskie Nauki 12 (1959).
[46] C.L. Yaws, P.K. Narasimhan, Chapter 1 – critical properties and acentric factor—organic compounds, in: Thermophysical Properties of Chemicals and Hydrocarbons, William Andrew Publishing, Norwich, NY, 2009, pp. 1–95, https://doi.org/10.1016/B978-081551596-8.50006-7.
[47] R.H. Perry, D.W. Green, J.O. Maloney, Perry's Chemical Engineering Handbook, 7th ed., McGraw-Hill, New York, 1997.
[48] K.P. Shen, M.H. Li, Solubility of carbon dioxide in aqueous mixtures of monoethanolamine with methyldiethanolamine, J. Chem. Eng. Data 37 (1992) 96–100, https://doi.org/10.1021/je00005a025.
[49] F.-Y. Jou, A.E. Mather, F.D. Otto, The solubility of CO2 in a 30 mass percent monoethanolamine solution, Canad. J Chem. Eng. 73 (1995) 140–147, https://doi.org/10.1002/cjce.5450730116.
[50] J.I. Lee, F.D. Otto, A.E. Mather, Equilibrium between carbon dioxide and aqueous monoethanolamine solutions, J. Appl. Chem. Biotech. 26 (1976) 541–549, https://doi.org/10.1002/jctb.5020260177.
[51] M. Wagner, I. von Harbou, J. Kim, I. Ermatchkova, G. Maurer, H. Hasse, Solubility of carbon dioxide in aqueous solutions of monoethanolamine in the low and high gas loading regions, J. Chem. Eng. Data 58 (2013) 883–895, https://doi.org/10.1021/je301030z.
[52] S. Kadiwala, A.V. Rayer, A. Henni, High pressure solubility of carbon dioxide (CO2) in aqueous piperazine solutions, Fluid Phase Equilib. 292 (2010) 20–28, https://doi.org/10.1016/j.fluid.2010.01.009.
[53] H. Li, Y. Le Moullec, J. Lu, J. Chen, J.C. Valle Marcos, G. Chen, F. Chopin, CO2 solubility measurement and thermodynamic modeling for 1-methylpiperazine/water/CO2, Fluid Phase Equilib. 394 (2015) 118–128, https://doi.org/10.1016/j.fluid.2015.03.021.
[54] L.P. Kyrides, F.C. Meyer, F.B. Zienty, J. Harvey, L.W. Bannister, Antihistaminic agents containing a thiophene nucleus, J. Am. Chem. Soc. 72 (1950) 745–748, https://doi.org/10.1021/ja01158a026.
[55] J.B. Matthews, J.F. Sumner, E.A. Moelwyn-Hughes, The vapour pressures of certain liquids, Trans. Faraday Soc. 46 (1950) 797–803, https://doi.org/10.1039/TF9504600797.
[56] J.G.M.S. Monteiro, D.D.D. Pinto, S.A.H. Zaidy, A. Hartono, H.F. Svendsen, VLE data and modelling of aqueous N, N-diethylethanolamine (DEEA) solutions, Int. J. Greenhouse Gas Control 19 (2013) 432–440, https://doi.org/10.1016/j.ijggc.2013.10.001.
[57] Y. Du, Y. Yuan, G.T. Rochelle, Volatility of amines for CO2 capture, Int. J. Greenhouse Gas Control 58 (2017) 1–9, https://doi.org/10.1016/j.ijggc.2017.01.001.